NASA CONTRACTOR REPORT





# AIR RADIATION GRAPHS:

## SPECTRALLY INTEGRATED FLUXES INCLUDING LINE CONTRIBUTIONS AND SELF ABSORPTION

*by Richard A. Allen*

*Prepared by*
AVCO CORPORATION
Everett, Mass.
*for*
ADVANCED RESEARCH PROJECTS AGENCY
*and*

NATIONAL AERONAUTICS AND SPACE ADMINISTRATION • WASHINGTON, D. C. • AUGUST 1966

NASA CR-556

# AIR RADIATION GRAPHS:

# SPECTRALLY INTEGRATED FLUXES INCLUDING LINE CONTRIBUTIONS AND SELF ABSORPTION

By Richard A. Allen



Prepared under Contract Nos. DA-01-021-AMC-12005(Z) and NASw-748 by
AVCO CORPORATION
Everett, Mass.

for

ADVANCED RESEARCH PROJECTS AGENCY

and

NATIONAL AERONAUTICS AND SPACE ADMINISTRATION

For sale by the Clearinghouse for Federal Scientific and Technical Information
Springfield, Virginia 22151 – Price $2.50

TABLE OF CONTENTS


| | Page |
|---|---|
| Abstract | v |
| INTRODUCTION | 1 |
| MOLECULAR RADIATION | 3 |
| FREE-BOUND AND FREE-FREE RADIATION | 9 |
| ATOMIC LINE RADIATION | 13 |
| ACKNOWLEDGMENT | 15 |
| REFERENCES | 48 |

## ABSTRACT

Calculations have been made of the equilibrium radiation emitted from air over a range of temperatures from 2,000°K to 23,000°K and over a density range from $10^{-6}$ to 10 atmospheres. The calculations are presented in graphical form and are in terms of the radiation flux emitted from one side of infinite slabs of finite thickness. The molecular band systems have been calculated using a smeared rotational model, and are carried out for a slab thickness of 1 cm. Atomic line and free-bound transitions are important contributors at elevated temperatures and also generally undergo significant amounts of self-absorption. Consequently calculations for these two classes of radiation have been made with slab thickness as an added parameter. The lines, free-bound and free-free radiation have also been split into the two spectral regions for the radiation flux above and below 2000 Å.

# INTRODUCTION

These tables have been designed primarily for making radiation heating estimates for re-entry into the earth's atmosphere, and consequently a conservative approach has been made commensurate with a fairly good understanding of the radiation physics. In the region where radiation heating is generally important free-bound and atomic line radiation are the important radiating mechanisms. Self-absorption of these two sources of radiation plays a significant role especially in the vacuum ultraviolet and must be included in realistic radiation calculations.

The calculations have been carried out for infinite air slabs of finite thickness since this geometry lends itself most readily to practical applications. For instance, radiation fluxes at the stagnation point of a vehicle estimated on the basis of an infinite slab approximation do not exceed the value based on better geometric considerations by more than about 15%.[1] This over-estimation is also quite compatible with the general accuracy to which oscillator strengths are known.

The line broadening formula used for the line radiation enables a relatively easy approach to calculating the fluxes from the lines although the use of it also tends to overpredict the radiation in the ultraviolet. The formulas developed for the free-bound radiation are hydrogen like for transitions in the visible and is a model which does fit reasonably well with shock tube and arc measurements. In order to account for non-hydrogen like behavior of transitions involving ground states of N we have used the calculated and measured value of $10^{-17}$ $cm^2$ with no wavelength dependence.

For the comparison of air data and calculations based on the methods used in this study, attention should be given to the references in Table I and in general, the calculations embody all the oscillator strengths and cross sections which we feel give the best phenomenological fit to air data.

# MOLECULAR RADIATION

## A. Diatomic Molecules

For the purposes of making these radiation tables,[2] we have made use of the expression developed by Keck[3] et al and Patch[4] for the radiation intensity emitted from an optically thin gas sample at the thermodynamic equilibrium. This expression is, after replacing the constants by their proper values:

$$\frac{dI}{dV\,d\Omega\,d\lambda} = 3.19\times10^{-34}\left|\frac{R(\bar{r})}{e\,a_o}\right|^2 N\,\phi\,\tilde{\nu}^6\,\frac{hc}{kT_r}\,e^{-\frac{hc\,\tilde{\nu}_{oo}}{kT_e}}\,\frac{w}{cm^3-\mu-ster} \qquad (1)$$

The symbols are as those given in Ref. 5 where $R(\bar{r})$ is the dipole matrix element for the transition and may be a function of the internuclear separation. $a_o$ is the radius of the first Bohr orbit and e is the charge of the electron. N is the number of molecules in the absorbing state which is not necessarily the ground state, and h, c, and k are the usual constants. $T_r$, $T_v$ and $T_e$ are the rotational, vibrational and electronic temperatures, respectively. The absorption oscillator strength is related to the matrix element by the expression,

$$f_{v''v'} = \left(\frac{\tilde{\nu}}{3\,R_\infty}\right)\left|\frac{R(\bar{r})}{e\,a_o}\right|^2 \qquad (2)$$

where $R_\infty$ is the Rydberg.

As used in formulas (1) and (2), the electronic transition moment, $\left|\frac{R(\bar{r})}{e\,a_o}\right|^2$ is related to the radiative lifetime for spontaneous emission, $\tau$, by the following expression

$$\frac{1}{\tau} = \frac{8\pi^2\,r_o\,c\,\tilde{\nu}_e^{\,3}\,g''}{3\,R_\infty\,g'}\left|\frac{R(\bar{r})}{e\,a_o}\right|^2 \qquad (3)$$

where g' and g'' are the electronic degeneracies of the upper and lower states respectively and

$$\tilde{\nu}^3_e = \sum_{v''} \tilde{\nu}^3 \, q_{v'v''} \tag{4}$$

Note should be made that the electronic transition moment has been defined differently by various authors[5, 6, 7, 8] the differences occuring in the way that the electronic degeneracies appear in the expression (3) that relates the lifetime for spontaneous emission to the electronic transition moment.

$\phi$ is called the spectral distribution function and gives the spectral details of the band system. It is calculated from a knowledge of the Frank Condon factors and the spectroscopic constants.

$$\phi = \frac{kT_r}{hc} \; \frac{1}{Q''_v \, Q''_r \, (B'_e - B''_e)} \sum_{\epsilon'_r \geq 0} q_{v'v''} \, e^{-\left(\frac{\epsilon'_v}{kT_v} + \frac{\epsilon'_r}{kT_r}\right)} \tag{5}$$

where: $Q''_v = \left[1 - \exp\left(-hc\,\omega''_e/kT_v\right)\right]^{-1}$ is the vibrational partition function for the absorbing state, (the ' refers to the excited electronic or emitting state, and the '' refers to lower electronic or absorbing state);

$Q''_r = kT_r/hc\,B''_e$ is the rotational partition function for the absorbing state;

$q_{v'v''}$ is the Condon factor for the transition from v' to v'';

$\tilde{\nu}_v = \omega_e\,(v + 1/2) - \omega_e\,x_e\,(v + 1/2)^2 + \omega_e\,y_e\,(v + 1/2)^3$ is the wave number of the $v^{th}$ vibrational level;

$\tilde{\nu}_{v'v''} = \tilde{\nu}_{oo} + (\tilde{\nu}_{v'} - \tilde{\nu}_{o'}) - (\tilde{\nu}_{v''} - \tilde{\nu}_{o''})$ is the wave number for the vibrational transition between states v' and v'';

$\epsilon_{v'} = hc\,(\tilde{\nu}_{v'} - \tilde{\nu}_{o'})$ is the vibrational energy relative to the ground vibrational state for the emitting state;

$\epsilon_{r'} = B_{e'}/(B_{e'} - B_{e''})\,hc\,(\tilde{\nu} - \tilde{\nu}_{v'v''})$ is the rotational energy for the emitting state, with the approximation made that the rotational quantum number J does not change in a given transition.

In a transition, J can change in emission by + 1, 0 or -1 giving R, Q and P branches, respectively. However, for increasing rotational temperatures where high J values are more heavily weighted or where the spectrum is observed with coarse resolution, the effect of $\Delta J \pm 1$ is washed out. The degree to which this approximation matches the detailed calculations for the rotational structure is discussed in reference 9. Although it lacks detail within an interval $\Delta \tilde{\nu} \approx B_e^2/\Delta B_e$ of the band head $\phi \tilde{\nu}^6$ gives a good description of the vibrational structure.

$\phi$ and related parameters were calculated for the various radiators which should contribute in air for $T_r = T_v = T_e$, and appear in references 2 and 9. These radiators along with the recommended oscillator strengths are listed in Table 1.

For the sake of simplicity and also because of the general lack of information to the contrary, no internuclear separation dependence for the electronic transition moments has been assumed in calculating the total radiation to be expected from the molecular band systems listed in Table I. The integration over wavelength was carried out by a computer program, which calculated $\phi \lambda^{-6}$ and integrated over wavelength. The computer output for these calculations are given in references 2 and 9. The reference sources for the oscillator strengths are also listed and are felt to be the best values to use although several of them are still open to question, notably those for the $N_2$ (1+) and $N_2$ Birge Hopfield systems. Measurements in pure $N_2$ give a value of 0.1 for the electronic transition moment for the $N_2$ (1+) system however a value of 1.0 in parenthesis in Table I was used since Wray[28] has found this value to use in order to best phenomenologically fit air data. An electronic transition moment of 1.4 for the $N_2$ $b\,'^1\Sigma \rightarrow X$ Birge Hopfield is used with no value assigned to the $b\,^1\Pi \rightarrow X$ transition; however we found that the best fit to the temperature dependence of the data of Wray[35] is given by assuming that the main $N_2$ component in the ultraviolet is the $b\,'^1\Sigma \rightarrow X$ transition. For discussions of the oscillator strengths pertaining to the other radiators attention should be given to the appropriate references in Table I.

The calculations for the band system in Figures 1 - 8 are carried out for the flux from one side of an infinite slab (i.e. $2\pi$ ster) of 1 cm

TABLE I

| Molecular Band Radiation | $\left\|\frac{R(\bar{r})}{ea}\right\|^2$ | $\tau$ sec | $f_{oo}$ | Ref. | Key |
|---|---|---|---|---|---|
| $N_2$ (1+) | .1 (1.0 Air) | $1.1 \times 10^{-5}$ | .003 | 5, 28 | 3 |
| $N_2$ (2+) | .7 | $2.7 \times 10^{-8}$ | .06 | 5 | 1 |
| $N_2$ Birge Hopfield #1 $b\ ^1\Pi \rightarrow X$ | | | | 32 | |
| $N_2$ Birge Hopfield #2 $b'\ ^1\Sigma \rightarrow X$ | 1.4 | $.71 \times 10^{-9}$ | .43 | 17, 32 | 2 |
| $N_2$ Lyman Birge Hopfield | $1.77 \times 10^{-5}$ | $1.7 \times 10^{-4}$ | $.37 \times 10^{-5}$ | 7 | 9 |
| $N_2^+$ (1-) | .45 | $.67 \times 10^{-7}$ | .035 | 5, 9 | 6 |
| $N_2^+$ (Meinel) | .45 | $3 \times 10^{-6}$ | .012 | 7, 34 | 7 |
| NO $\beta$ | .08 | $.67 \times 10^{-6}$ | .01 | 5 | 4 |
| NO $\gamma$ | .025 | $1.16 \times 10^{-7}$ | .003 | 5 | 5 |
| $O_2$ Schumann-Runge | 0.5 | $.82 \times 10^{-8}$ | .075 | 5 | 8 |
| NO Infrared Bands | | | | 33 | 13 |
| $NO_2$ Thermal | | | | 29 | 15 |
| $NO_2$ Recombination | | | | 29 | 14 |

| Electron Recombination and Scattering Radiation | | | |
|---|---|---|---|
| $N^+ + e \rightarrow N + h\nu$<br>$O^+ + e \rightarrow O + h\nu$ | Hydrogen like model with Bethe & Salpeter continuum $\bar{f}$ numbers and photoionization cross section of $10^{-17}$ $cm^2$ for 2 p states | 17, 18 | 12 |
| $N^+ + O^+$ free free | Unsold expression with effective $Z^2$ of 1.5 | 17 | 12 |
| $N^{++} + O^{++}$ fb + ff | Unsold expression with effective $Z^2$ of 4 | | 18 |
| $O + e \rightarrow O^- + h\nu$ | Photoionization cross sections | 30 | 10 |
| $N_2$ ff | Unsold expression with $Z^2 = .022$ | 31 | 16 |
| $N_{ff}$ | Unsold expression with $Z^2 = .009$ | 31 | 17 |

| Atomic Line Radiation | | |
|---|---|---|
| N, O | 26 | 11 |

thickness and also with the assumption that the band systems are optically thin until they are cut off by the blackbody. This simplification can lead to an over-estimation of radiation fluxes when the total gas emissivity calculation approaches unity and when the average line width to spacing ratio is small.

Fairbairn[10] has performed a detailed line by line calculation over several sequences of the CN and $C_2$ violet systems with the line width and shape as a parameter, and this is an example of the type of calculation which is needed to properly account for self-absorption of band systems when gas emissivities are near unity.

The species concentrations which were used in order to perform these radiation calculations are from the data published in reference 11 for temperatures up to 15,000°K and reference 12 for temperatures up to 24,000°K.

B. $NO_2$ Radiation

Radiation from $NO_2$ comes about by two processes. One that produced by an O atom recombination with NO forming $NO_2$ and a photon and also $NO_2$ radiating from an electronic transition. We have chosen the formulas given by Leavitt[13] to describe the radiation from these two sources.

## FREE-BOUND AND FREE-FREE RADIATION

### A. $N^+$ and $O^+$ Radiation

A calculation procedure was developed which used the continuum oscillator strengths of Bethe and Salpeter[13] to make the free-bound radiation predictions for $N^+$ and $O^+$ for all transitions emitting at a wavelength longer than 2000 Å. This calculation procedes on the basis that at thermodynamic equilibrium the emission can be related to the blackbody intensity by the photoabsorption coefficient, and that the excited electronic states of N and O can be approximated by a hydrogen like model.

The classical wave number dependence for a hydrogen photo-absorption edge is $\frac{1}{\tilde{\nu}^3}$. The f sum rule also states that $\int \sigma d\tilde{\nu} = \pi r_o f$ where $r_o$ is the classical electron radius and f is the oscillator strength. Therefore,

$$\sigma = 2\pi r_o \frac{\tilde{\nu}^2_{n\ell} \bar{f}_{n\ell}}{\tilde{\nu}^3} \tag{6}$$

where $\tilde{\nu}_{n,\ell}$ is the wave number of the photoabsorption edge of atomic state $n,\ell$ and $\bar{f}_{n\ell}$ is the continuum oscillator strength of state of principal quantum number, n, and azimuthal quantum number, $\ell$. Energy levels for allowed transitions of the bound electron going to a free electron and the ion in its ground state were taken from the tables of Moore[14] to locate the position of photoabsorption edges. The continuum oscillator strengths in conjunction with equation (6) were used to obtain the photoabsorption cross section for each level of the atom versus wave number. Contributions from all levels were then summed. The continuum oscillator strengths for all n states less than 5 were from Bethe and Salpeter, and for all other states the following expression was used with the constraint that $\bar{f}$ must be equal to or less than 1.

$$\overline{f}_{n\ell} = \frac{16\,R^2}{3\sqrt{3}\,\pi\,\tilde{\nu}^2_{n\ell}(2J+1)\,n^3} \tag{7}$$

Formula (7) can be obtained from the usual expression for the free-bound cross absorption cross section for hydrogen[15] and equation (6). $\tilde{\nu}_{n,\ell}$ is the wave number of the photoabsorption edge for a given state, J and n are the inner and principle quantum numbers, respectively. R is the Rydberg expressed in wave numbers.

From the photoionization cross section, the radiation emitted from an equilibrium optically thin gas sample of thickness L over $2\pi$ ster is

$$\frac{dI}{dV\,d\tilde{\nu}\,d\Omega} = 2\pi\,N_{n,\ell}\,\sigma_{n,\ell}\,BB_{\tilde{\nu}\perp}\,(1-e^{-hc\,\tilde{\nu}/kT}) \tag{8}$$

$BB_{\tilde{\nu}\perp}$ is the blackbody intensity perpendicular to the surface and $(1-e^{-hc\,\tilde{\nu}/kT})$ is the factor which properly accounts for induced emission. $\pi BB_{\tilde{\nu}\perp} = BB_{\tilde{\nu}}$ where $BB_{\tilde{\nu}}$ is the blackbody intensity radiated from a surface over $2\pi$ ster. h and c are the usual constants, $N_{n,\ell}$ is the concentration of absorbing atoms in state $n,\ell$ and $\sigma_{n,\ell}$ is the photoabsorption cross section of state $n,\ell$. A computer program was written to calculate the free-bound radiation from optically thin samples of $N^+$ and $O^+$ using the procedure outlined above.

A comparison between such a calculation and the Unsold[16] expression for the sum of the free-bound and free-free ion radiation

$$\frac{dI}{dV\,d\tilde{\nu}\,d\Omega} = 1.63 \times 10^{-35}\,T^{-1/2}\,N_e\,N_i\,Z^2 \quad \frac{W}{cm^2\ ster} \tag{9}$$

with an effective $Z^2$ of 1 is shown in reference 17. Predictions for the visible continuum radiation from air using this calculation procedure are in reasonable agreement with measurements.[17] In the vacuum ultraviolet however, free-bound transitions in air involve ground states or near ground states for the absorbing atom. These electronic states are least likely to

be coulombic and are also states which have equivalent electrons. The hydrogen-like oscillator strengths are therefore not applicable to these transitions for N and O although they are reasonable to use in predicting free-bound transitions occurring at longer wavelengths. This fact seems to be born out by the shock tube data obtained in the visible.[17] We have chosen to use a photoabsorption cross section for all allowed transitions from 2p states of N and O to be $10^{-17}$ $cm^2$ with no wavenumber dependence. Bates and Seaton[18] calculate approximately this value for the ground atomic state of N and a similar value has been inferred from measurements by Ehler & Weissler.[19] The radiation flux calculations for most gas conditions and geometries was not very sensitive to what cross section was used for photoionization of O in the vacuum ultraviolet. All allowed free-bound transitions for O involving the recombination of an electron and $O^+$ in the 2p states occur at wavelengths below 910 Å. This wavelength region is not only dominated by $N^+ + e$ processes but in situations where radiation heating is important is also usually strongly self absorbed. Consequently, the radiation is limited by the blackbody intensity.

Self absorption serves to reduce the free-bound radiation in the ultraviolet under many conditions over the spectral region covering the 2p photoabsorption edges of N. Use has been made of the expression of Olfe[20] which relates the flux from one side of an infinite gas slab to a continuous absorption coefficient. The results of calculations for the radiation emitted in two spectral regions are given in figures 9 - 32 for the region below and above 2000 Å respectively. The growth curve of total intensity with slab thickness does not obey a simple growth law since part of the spectrum is optically thin while part is not, consequently the results are given with slab thickness as a parameter.

B. $N^{++}$ and $O^{++}$ Radiation

At the higher temperatures and lower densities calculated for these radiation tables, the air is sufficiently doubly ionized that the radiation produced by electrons being captured and decelerated by $N^{++}$ and $O^{++}$ becomes important. This radiation was calculated by use of expression (9) using an effective Z of 2 and carrying out the integration over wavenumber to the vacuum ultraviolet photoabsorption edges of N.

C. $O^-$ and $N^-$ Continuum

The $O^-$ continuum was calculated using the photoabsorption cross sections measured by Branscomb and Smith. Measurements of the photoabsorption cross section for $N^-$ ($^1D$) are still in question and calculations of the radiation from this source are not included.

D. Free-free Radiation from $N^+$ and $O^+$

The free-free contributions to the total radiation were calculated using the classical expression[16]

$$\frac{dI}{dV\, d\tilde{\nu}\, d\Omega} = 1.63 \times 10^{-35}\, T^{-1/2}\, N_e\, N_i\, Z^2\, e^{-\frac{hc\tilde{\nu}}{kT}} \quad \frac{W}{cm^2\ ster} \qquad (10)$$

Measurements obtained by Wilson[17] in the infrared were used to infer an effective $Z^2$ of 1.5 for this source of radiation for air. The contributions from this source are included with the curves labelled 12 in figures 1 - 8.

E. Free-free Radiation from $N_2$ and N

Taylor has measured the effective $Z^2$ for scattering of electrons from neutral $N_2$ of .022 and from N of .009. These values are used in conjunction with expression (10) to predict the curves labelled 16 and 17 respectively.

## ATOMIC LINE RADIATION

The total intensity of an optically thin spectral line emitted from one side of an infinite slab of thickness L is

$$I = \left[N_{n,\ell}\right] L\, 2\, \pi^2\, f\, r_o\, BB_{\tilde{\nu}\perp}\left(1-e^{-\frac{hc\,\tilde{\nu}}{kT}}\right) \qquad (11)$$

where $N_{n,\ell}$ is the number of atoms per unit volume in the absorbing state for the transition, f is the absorption bound-bound oscillator strength, $r_o$ is the classical electron radius, $BB_{\tilde{\nu}\perp}$ is the blackbody intensity perpendicular to the surface and $(1-e^{-hc\,\tilde{\nu}/kT})$ is the induced emission term.

In many situations, these lines undergo a certain amount of self-absorption which reduces the total measured intensity from the completely optically thin situation. In order to calculate the self-absorption, one must know the principal broadening mechanisms in the gas.[21] The line width and shape are the pertinent parameters which must be known. Lines also undergo a small wavelength shift for certain types of broadening, however, for the purposes of making these radiation tables this shift has been disregarded since it has little effect on the results. For the densities and temperatures considered in these calculations, Doppler and electron broadening mechanisms dominate over natural and pressure broadening by neutrals.

For the purposes of making calculations for these radiation graphs, shown in Figs. 9-32, the electron impact formula of Armstrong[21] and Stewart and Pyatt[23] was used. The total line half width is given in reciprocal centimeters by

$$W_{\tilde{\nu}} = 5.7 \times 10^{-16}\, N_e\, \frac{n^4}{Z^2}\, T^{-1/2}\ \mathrm{cm}^{-1} \qquad (12)$$

where $N_e$ is the electron density, n is the principle quantum number of the upper state, Z is the total charge of the atom minus one and T is the

temperature. Self-absorption of Lorentz, or dispersion shaped, non-overlapping lines, is treated by various authors[20, 24, 25]. For our purposes, we followed the definition of Penner[24] and Plass[25] for f(x) where f(x) is the function which describes the growth of intensity of a self-absorbed dispersion shaped line as a function of x.

$$x = \frac{\left[N_{n,\ell}\right] f\, r_o\, L}{W_{\tilde{\nu}}} =$$

$$\frac{N_{n,\ell}\ f r_o\ Z^2\ T^{1/2}}{5.7 \times 10^{-16}\ N_T\ n^4} \cdot \frac{N_T}{N_e} L = K \frac{N_T}{N_e} L \qquad (13)$$

f (x) versus $K \frac{N_T}{N_e} L$ was modified according to the work of Olfe[20] so as to be able to treat self-absorption for line radiation from one side of an infinite slab.

The line transitions listed by Griem[26] along with their f numbers includes most of the significant transition in N and O and were the ones used to set up a computer program to calculate the line contributions to the total radiation in two spectral regions, separated at 2000 Å and also carried out with slab thickness as a parameter. The assumption was made that all lines were non overlapping and also that the contribution from the lines not listed in Griem were not significant contributors to the total radiation.

The line widths as predicted by expression (12) were larger than doppler widths except at low temperatures and at low densities both regions where line radiation was not an important contributor or at a density where self-absorption effects were not large. Therefore only electron impact broadening was considered.

The calculations of the line radiation especially in the ultraviolet are open to the criticism that not enough self-absorption was included. The reason for this is that the electron impact widths as predicted by expression (12) are too large for the nitrogen line transitions occuring in the ultraviolet and visible regions of the spectrum. Stampa[27] has made nitrogen line width measurements on arcs which show that the approximation formula used in these calculations overpredicts the line widths by a factor

from approximately 4 to 9. Neglecting the doppler shape, this means that for situations where significant self-absorption is taking place, namely in the vacuum ultraviolet, the present radiation calculations would overpredict the radiation by a factor ranging from 2 to 3. The radiation emitted from one side of infinite gas slab from a strongly self-absorbed Lorentz shaped line varies as the square root of the half width. Since Doppler broadening is present, the overestimation is not as bad as a factor of 2 to 3 and for the purposes of making engineering numbers for radiation heating the present radiation calculations are reasonable.

## ACKNOWLEDGMENT

Credit is given to the many members of the Avco-Everett Research Laboratory, especially, A. Fairbairn, J. C. Keck, B. Kivel, P. Rose, R. Taylor, K. Wray, and L. Young, who gave many valuable suggestions and to B. Kaplan, A. Textoris, and T. Tsika who aided in much of the compilation of the results.

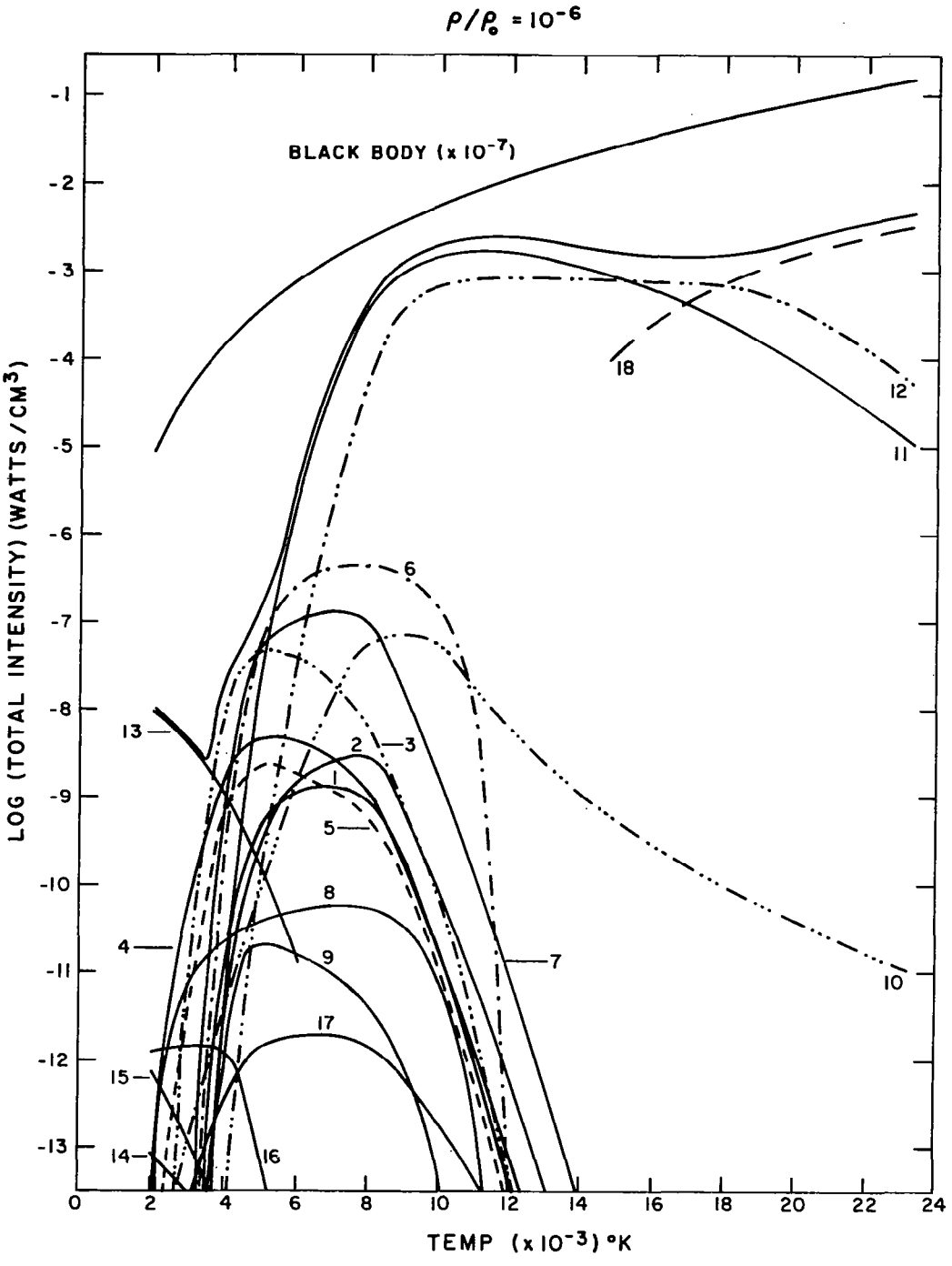


Fig. 1 Radiation calculations for the flux from one side of an infinite air slab 1 cm thick at a density of $10^{-6}$ atmospheric.

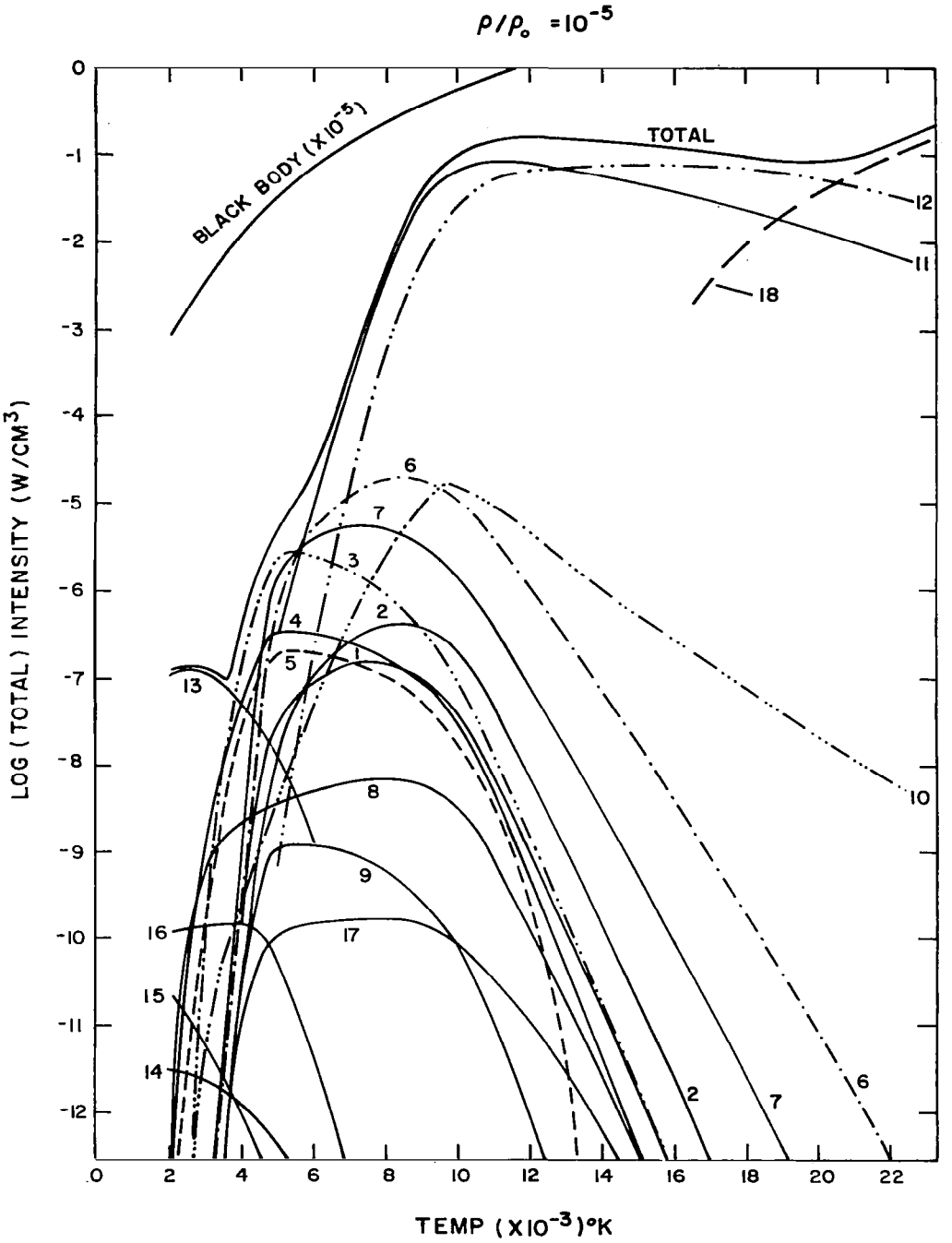


Fig. 2 Radiation calculations for the flux from one side of an infinite air slab 1 cm thick at a density of $10^{-5}$ atmospheric.

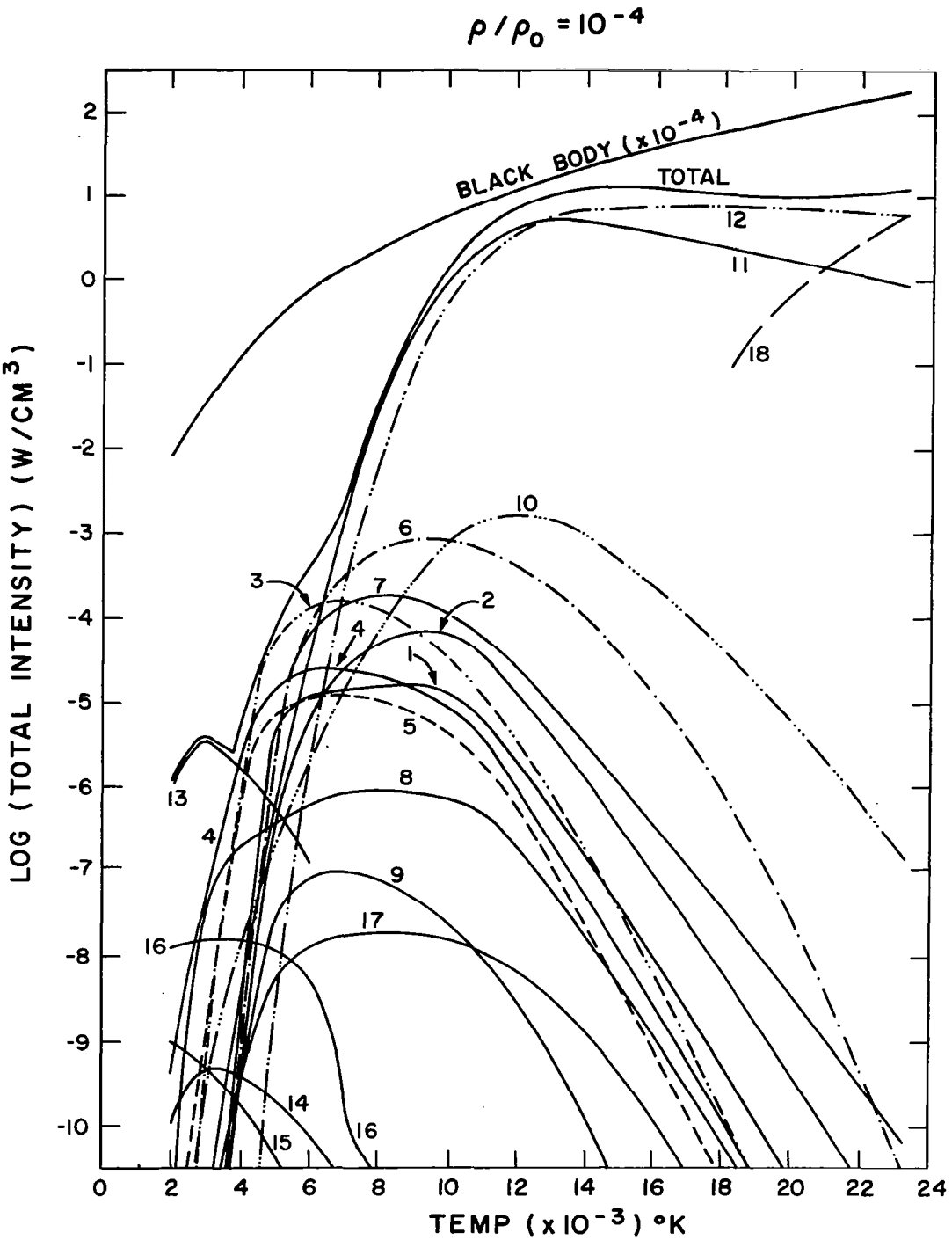


Fig. 3 Radiation calculations for the flux from one side of an infinite air slab 1 cm thick at a density of $10^{-4}$ atmospheric.

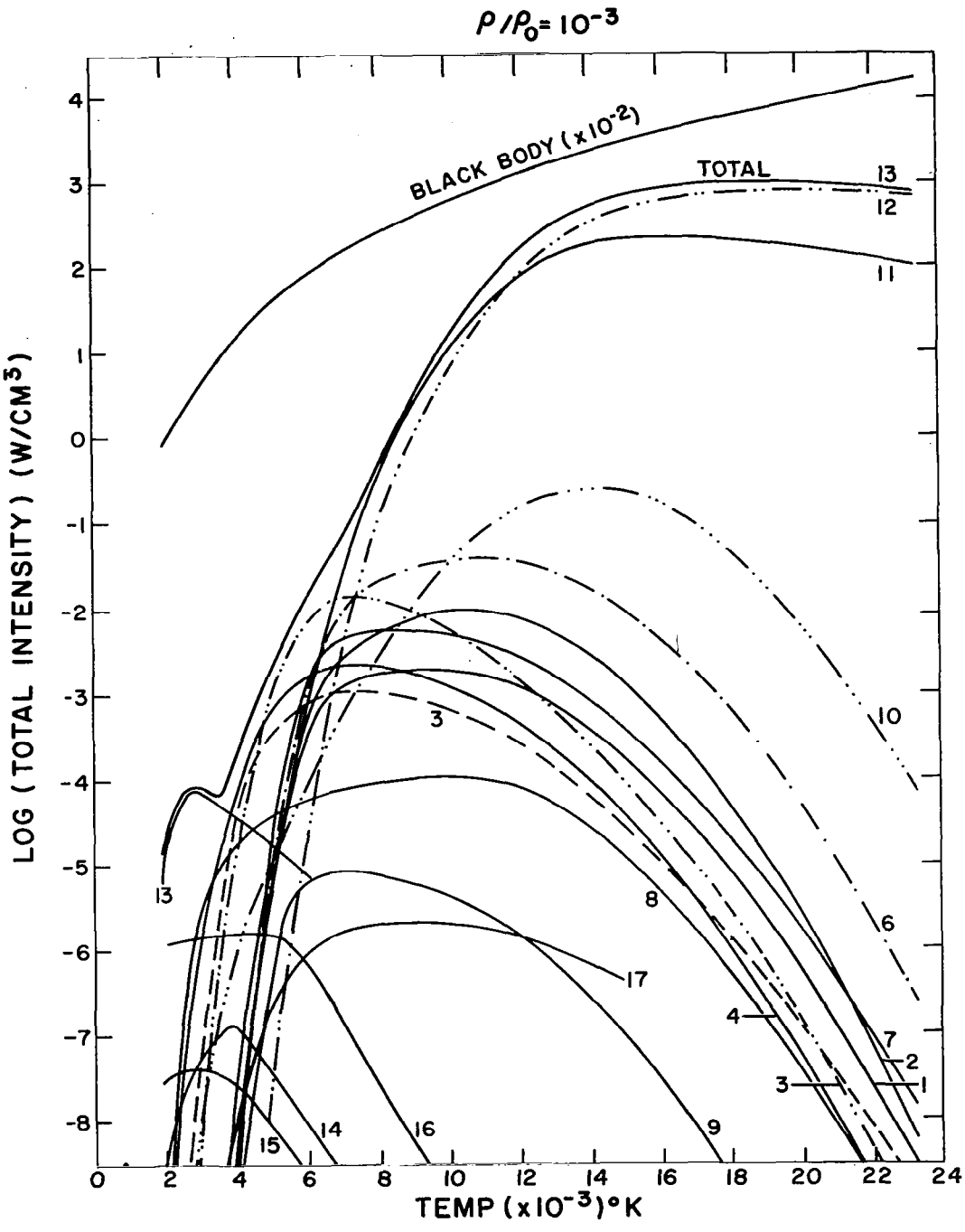


Fig. 4 Radiation calculations for the flux from one side of an infinite air slab 1 cm thick at a density of $10^{-3}$ atmospheric.

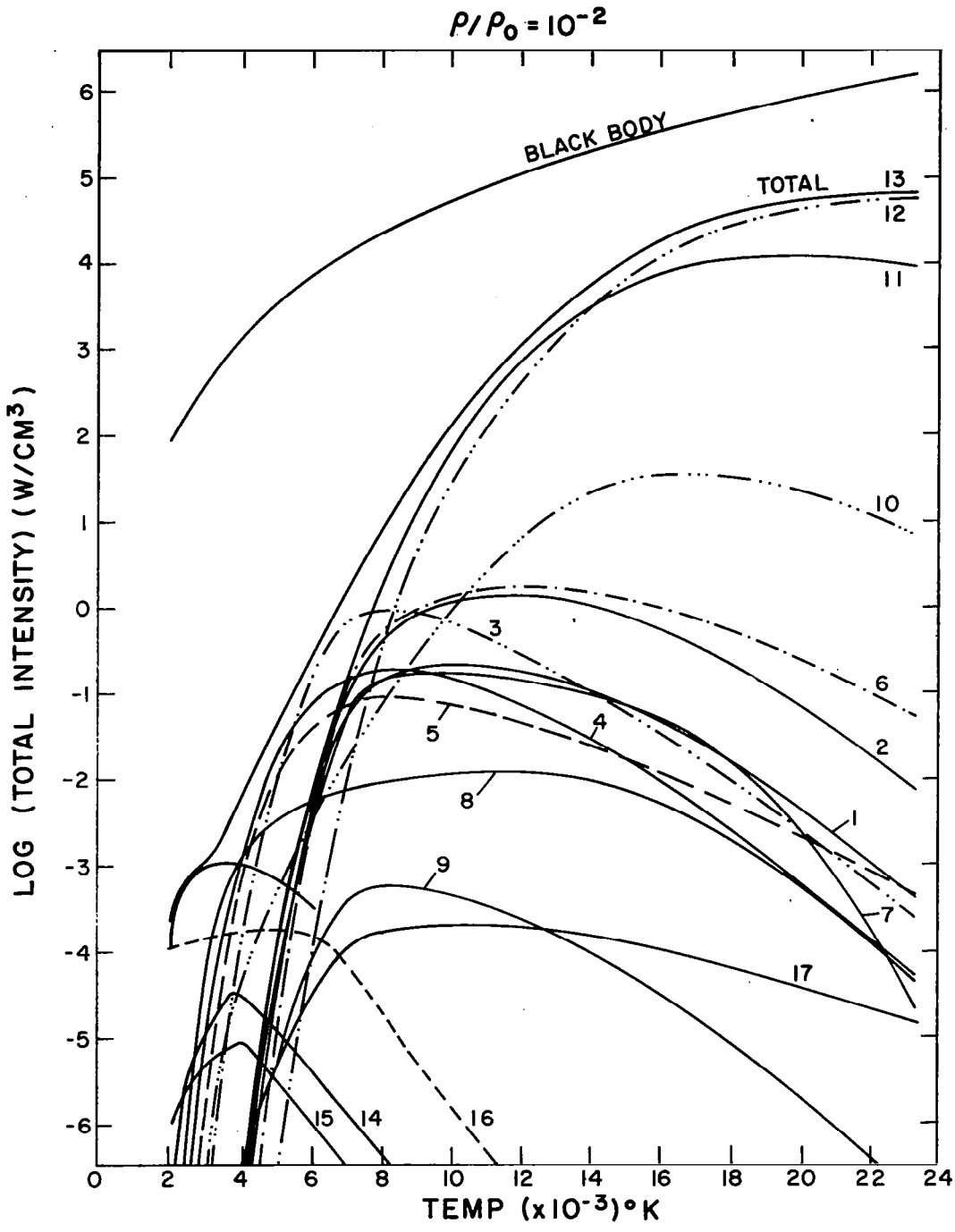


Fig. 5 Radiation calculations for the flux from one side of an infinite air slab 1 cm thick at a density of $10^{-2}$ atmospheric.

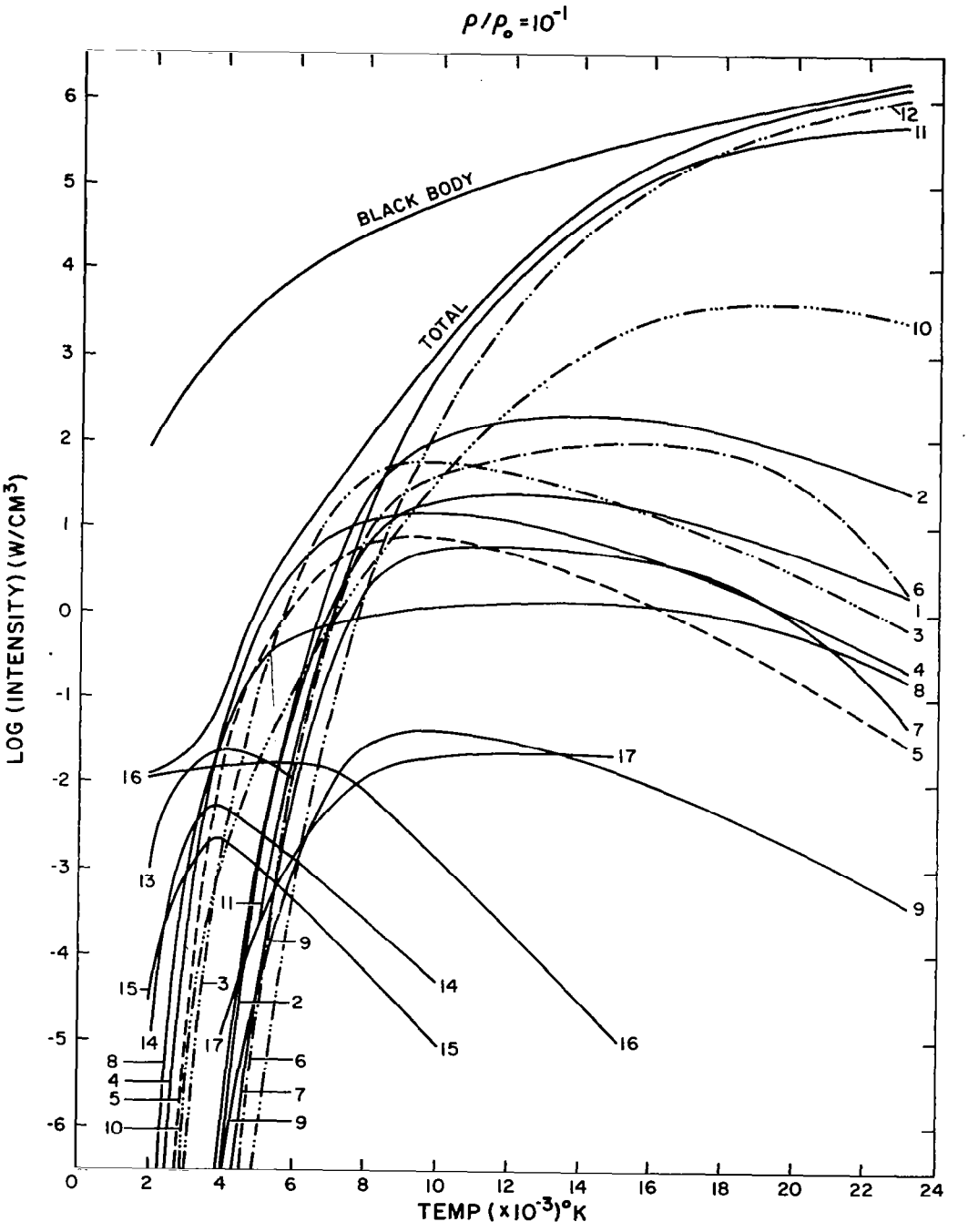


Fig. 6 Radiation calculations for the flux from one side of an infinite air slab 1 cm thick at a density of $10^{-1}$ atmospheric.

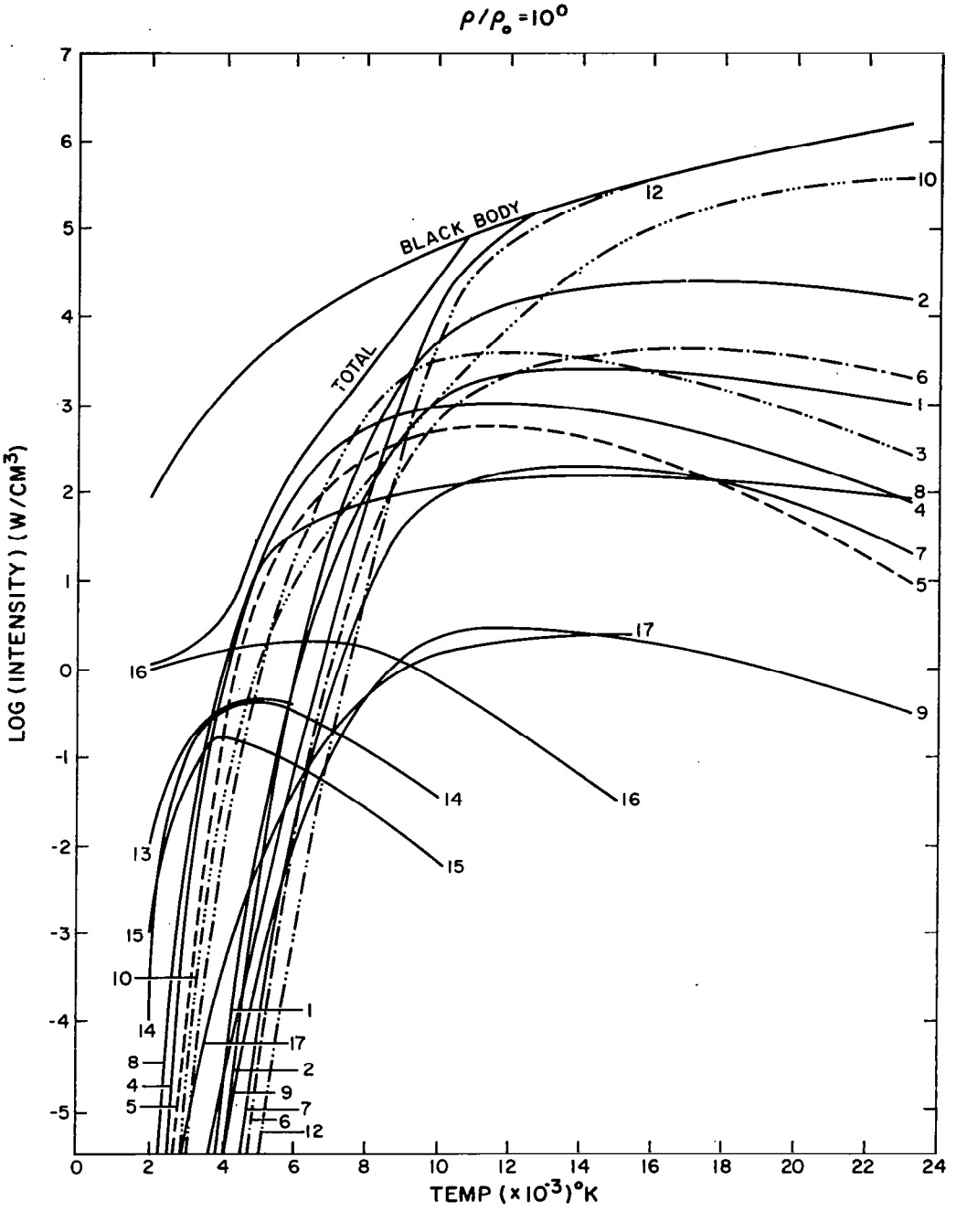


Fig. 7 Radiation calculations for the flux from one side of an infinite air slab 1 cm thick at a density of $10^{0}$ atmospheric.

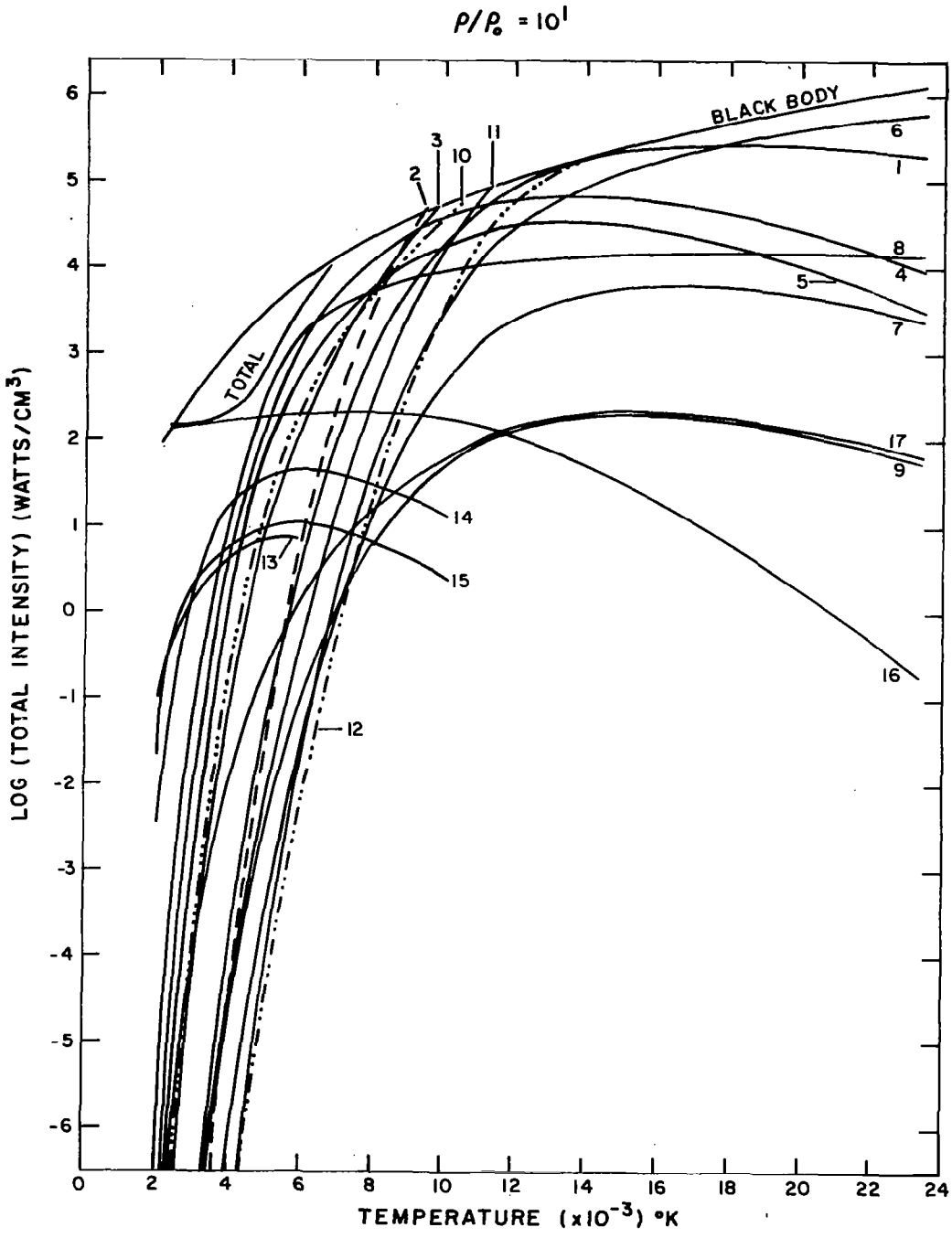


Fig. 8 Radiation calculations for the flux from one side of an infinite air slab 1 cm thick at a density of $10^1$ atmospheric.

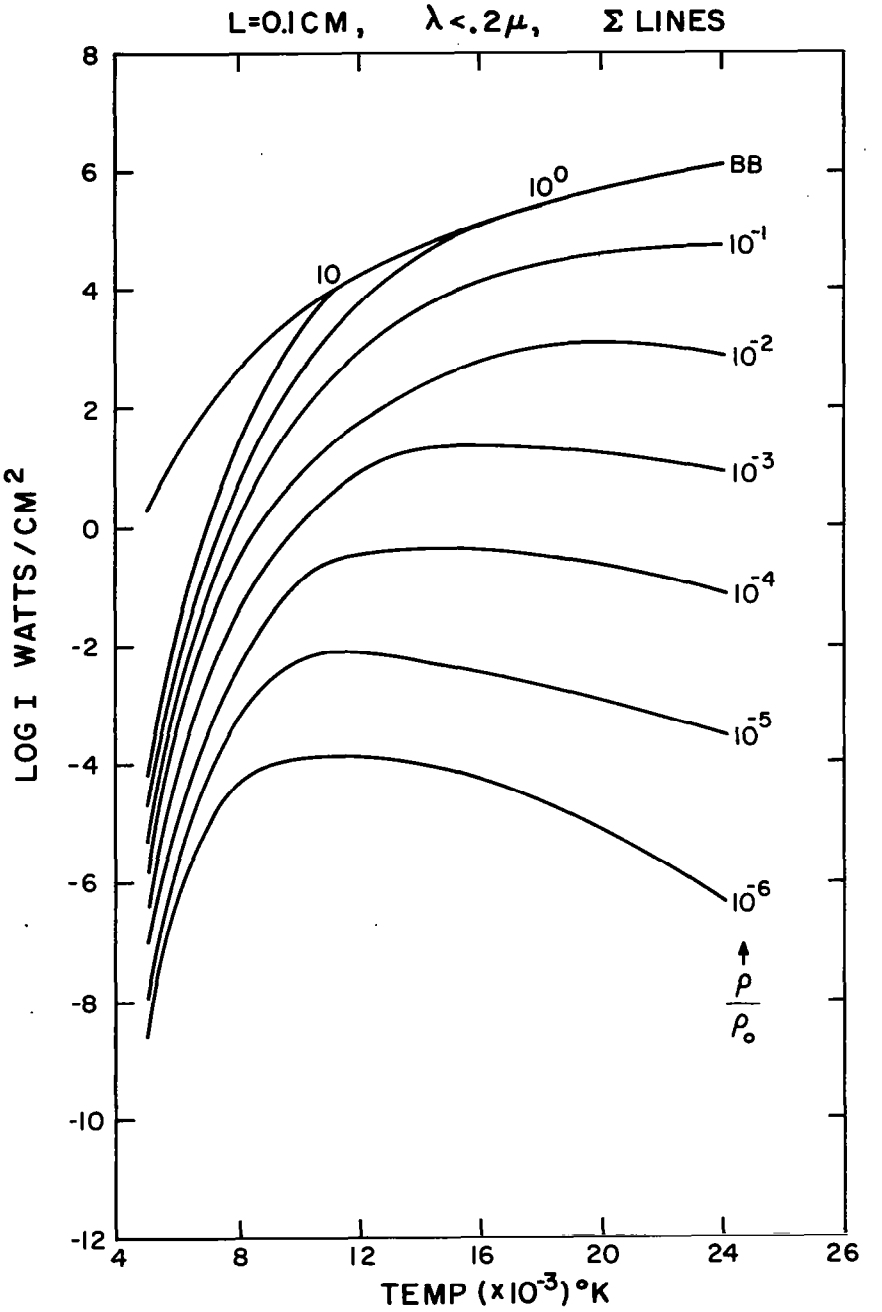


Fig. 9 Atomic nitrogen and oxygen line radiation flux from one side of an infinite air slab 0.1 cm thick for wavelengths less than 0.2 $\mu$.

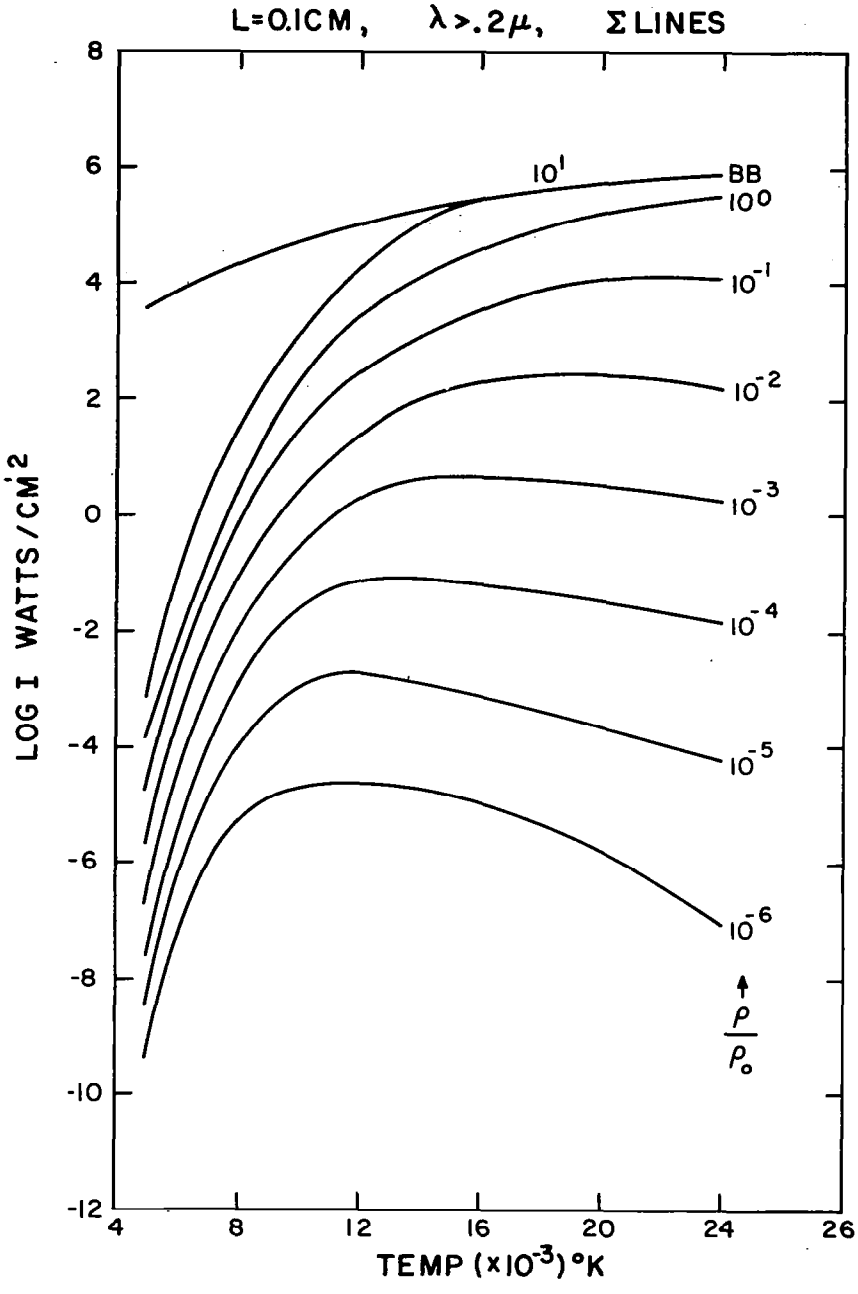


Fig. 10 Atomic nitrogen and oxygen line radiation flux from one side of an infinite air slab 0.1 cm thick for wavelengths longer than 0.2 $\mu$.

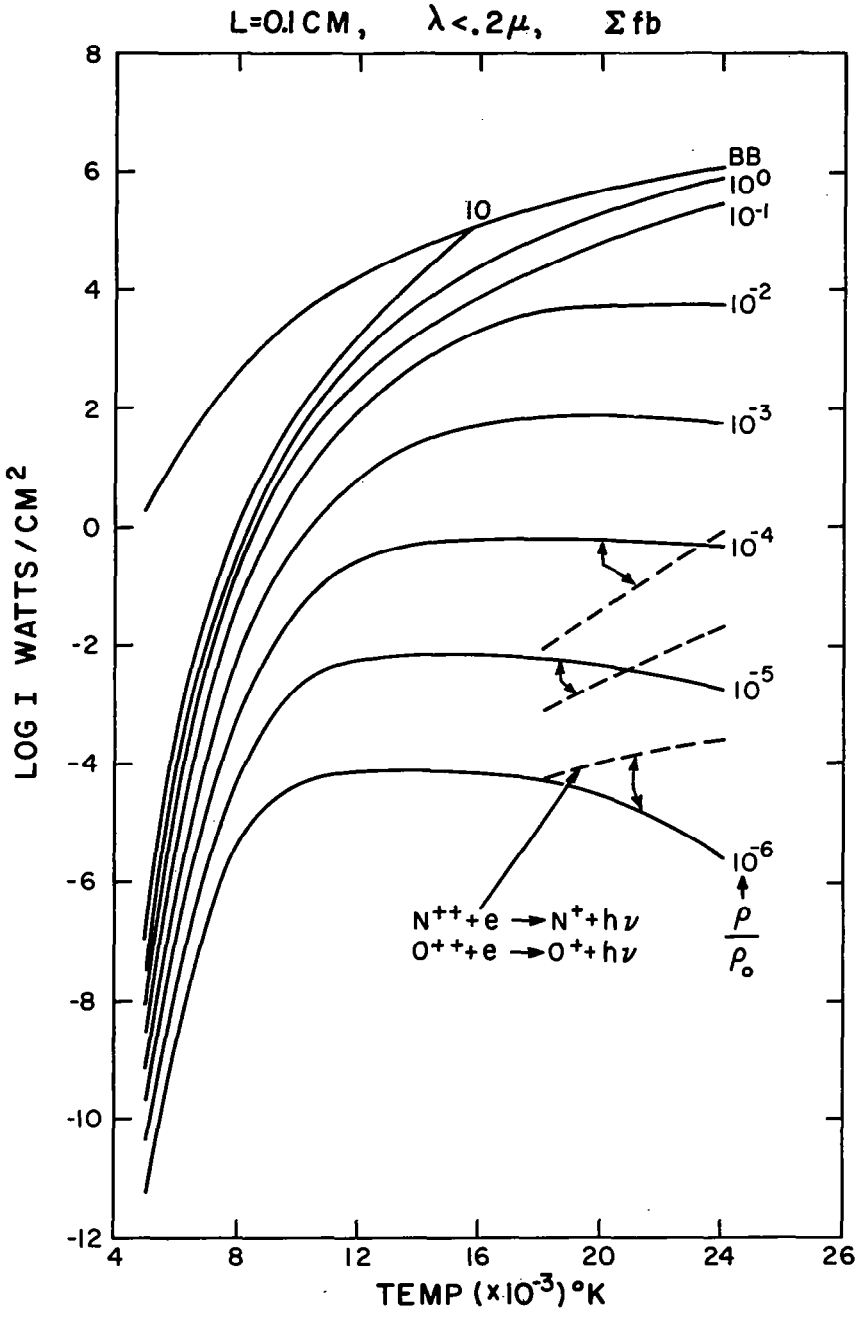


Fig. 11 Nitrogen and oxygen ion free bound radiation flux from one side of an infinite air slab 0.1 cm thick for wavelengths less than 0.2 $\mu$. The dashed lines are for the contributions from the $N^{++}$ and $O^{++}$.

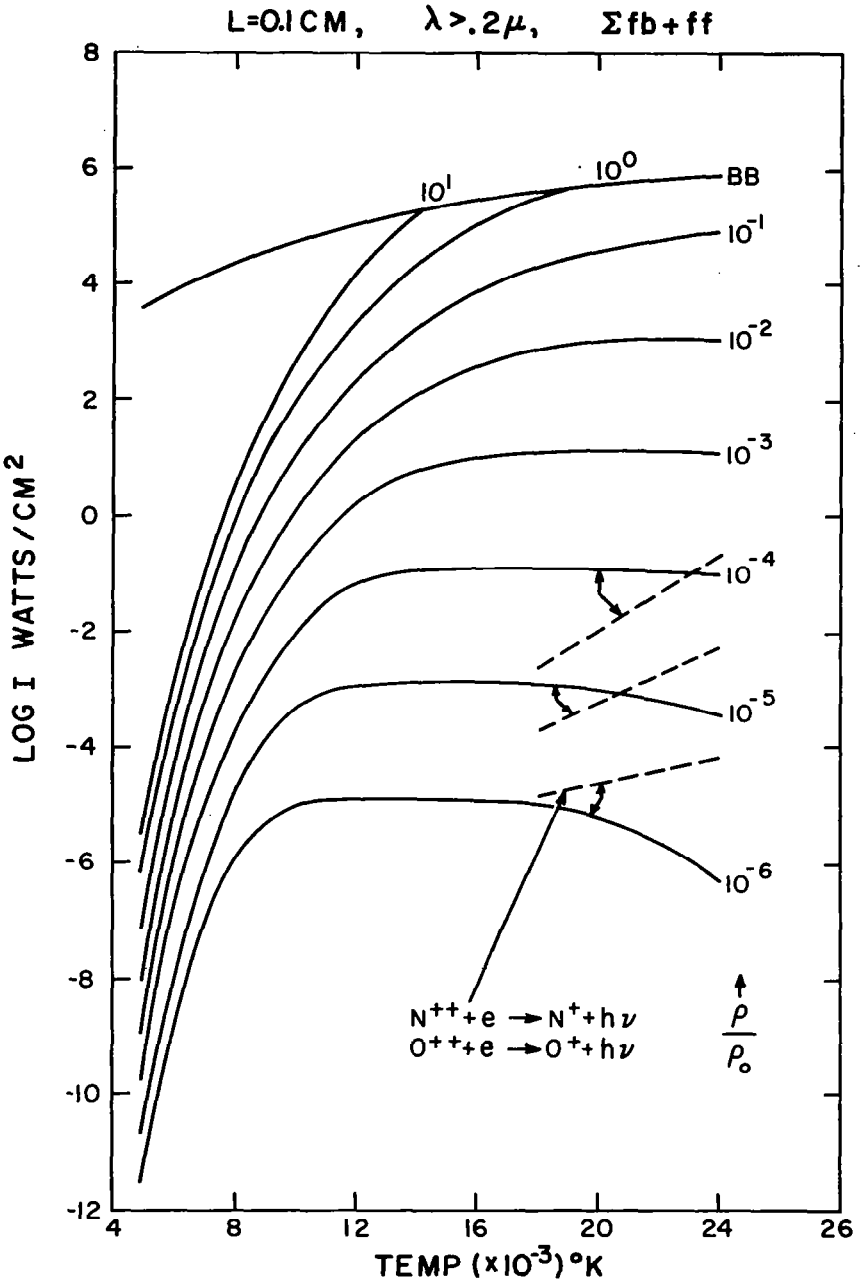


Fig. 12 Nitrogen and oxygen ion free bound and free free radiation flux from one side of an infinite air slab 0.1 cm thick for wavelengths greater than 0.2 $\mu$. The dashed lines are for the contribution from $N^{++}$ and $O^{++}$.

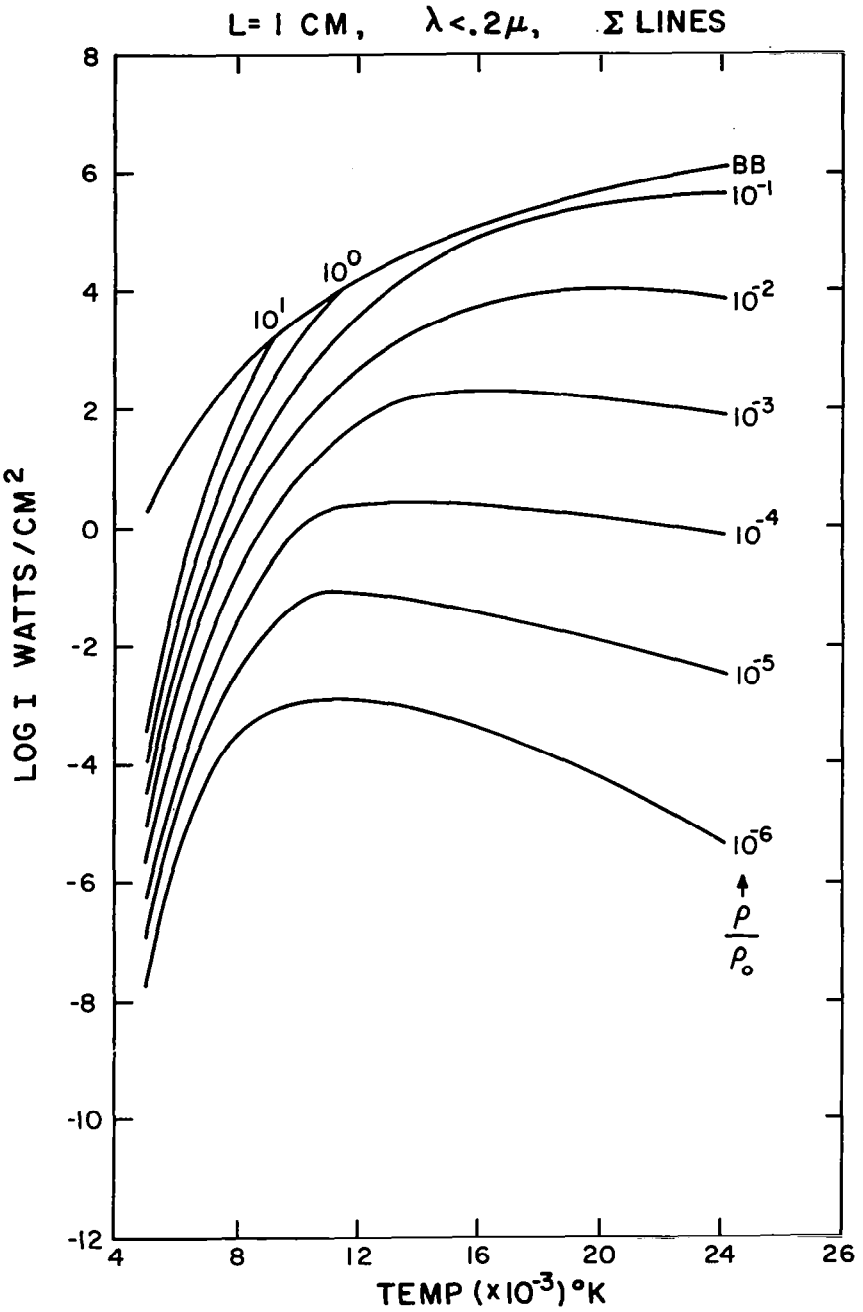


Fig. 13 Atomic nitrogen and oxygen line radiation flux from one side of an infinite air slab 1.0 cm thick for wavelengths less than 0.2 $\mu$.

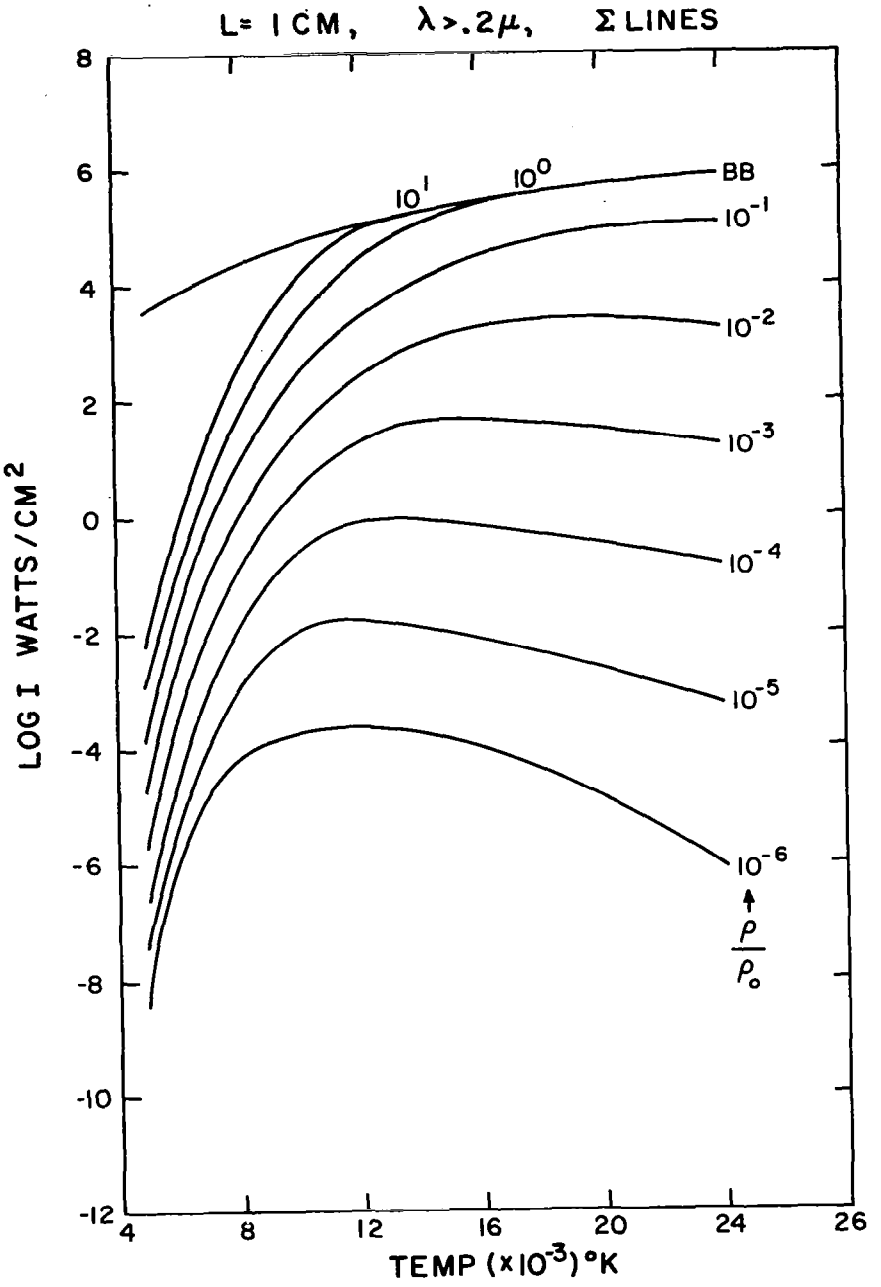


Fig. 14 Atomic nitrogen and oxygen line radiation flux from one side of an infinite air slab 1.0 cm thick for wavelengths longer than 0.2 $\mu$.

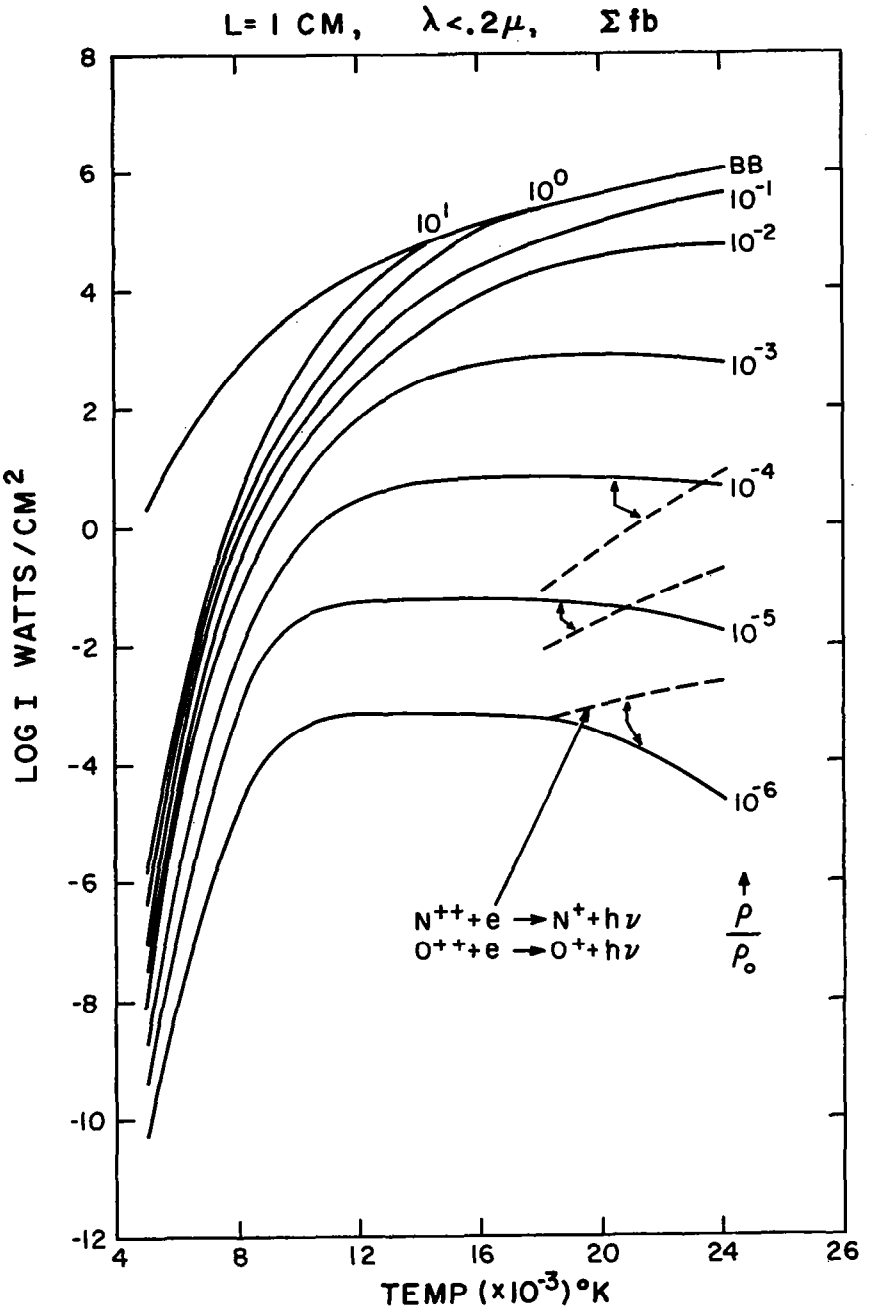


Fig. 15 Nitrogen and oxygen ion free bound radiation flux from one side of an infinite air slab 1.0 cm thick for wavelengths less than 0.2 $\mu$. The dashed lines are for the contributions from the $N^{++}$ and $O^{++}$.

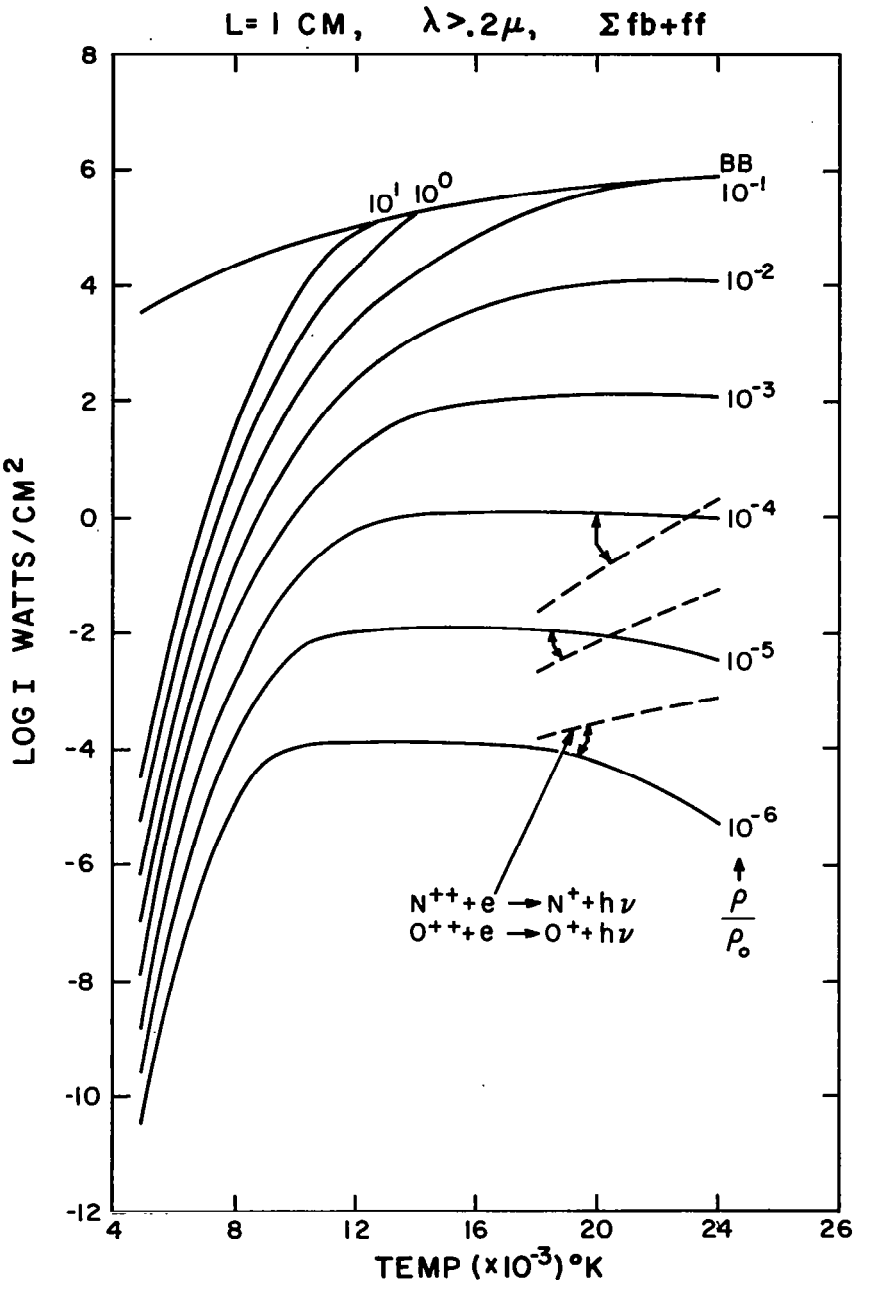


Fig. 16 Nitrogen and oxygen ion free bound and free free radiation flux from one side of an infinite air slab 1.0 cm thick for wavelengths greater than 0.2 $\mu$. The dashed lines are for the contribution from $N^{++}$ and $O^{++}$.

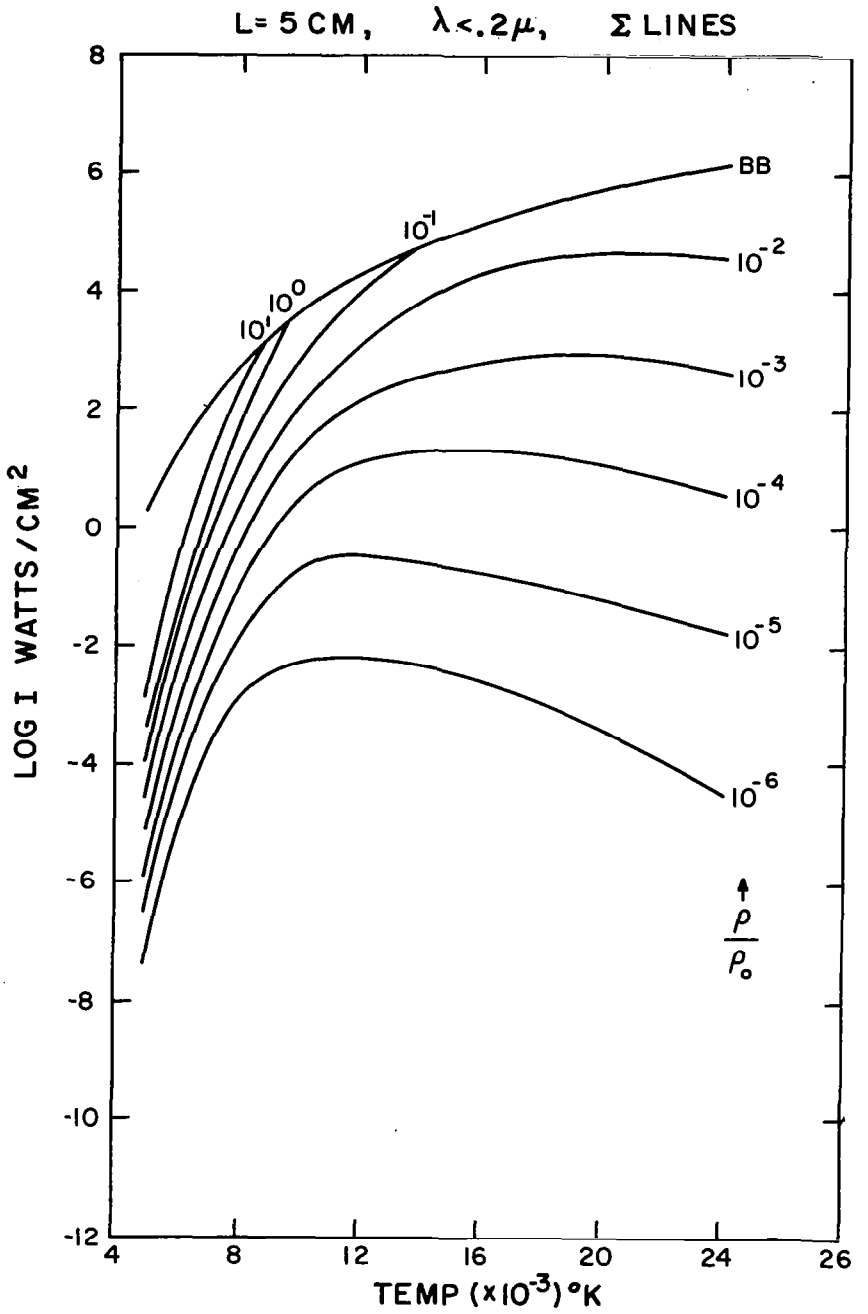


Fig. 17 Atomic nitrogen and oxygen line radiation flux from one side of an infinite air slab 5 cm thick for wavelengths less than 0.2 $\mu$.

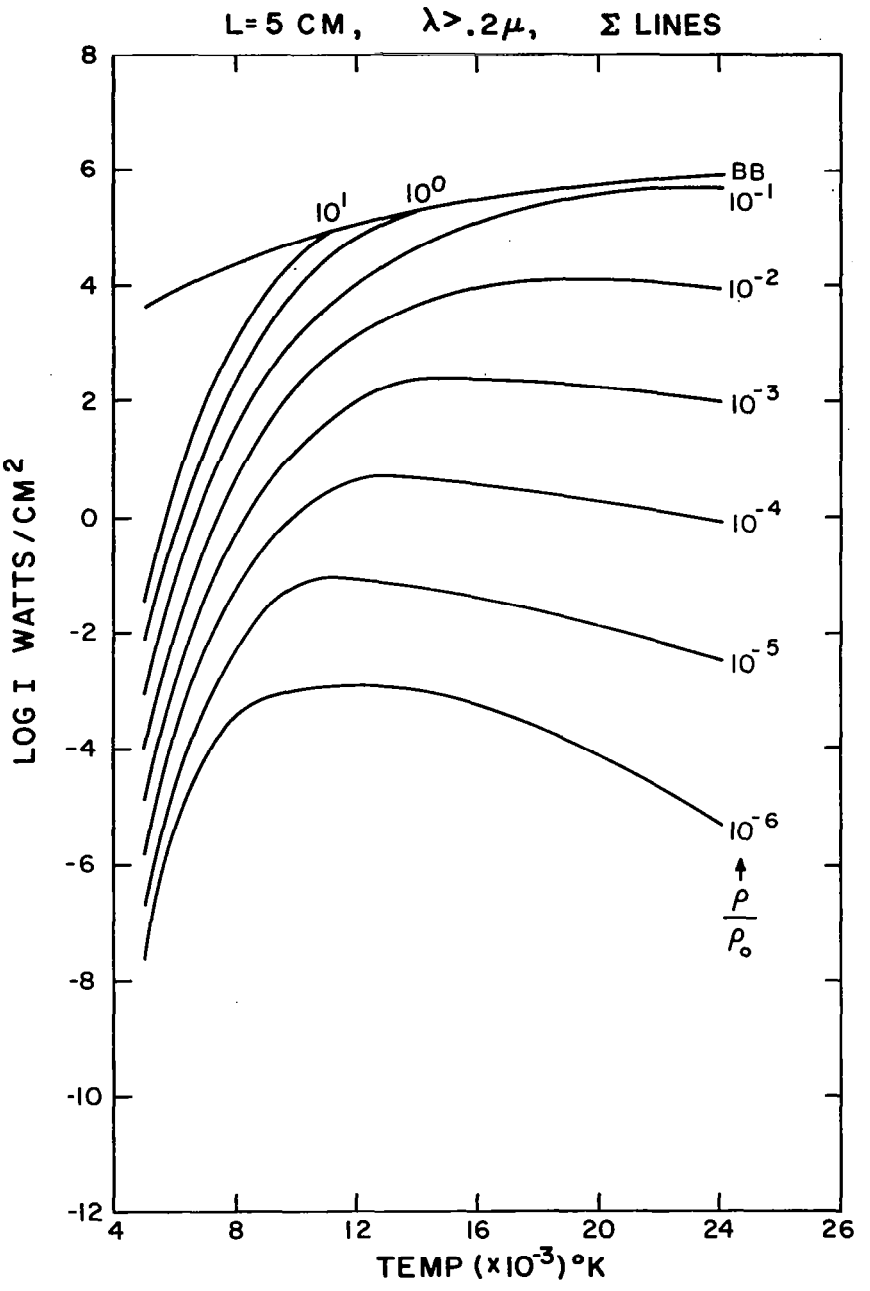


Fig. 18 Atomic nitrogen and oxygen line radiation flux from one side of an infinite air slab 5 cm thick for wavelengths longer than 0.2 $\mu$.

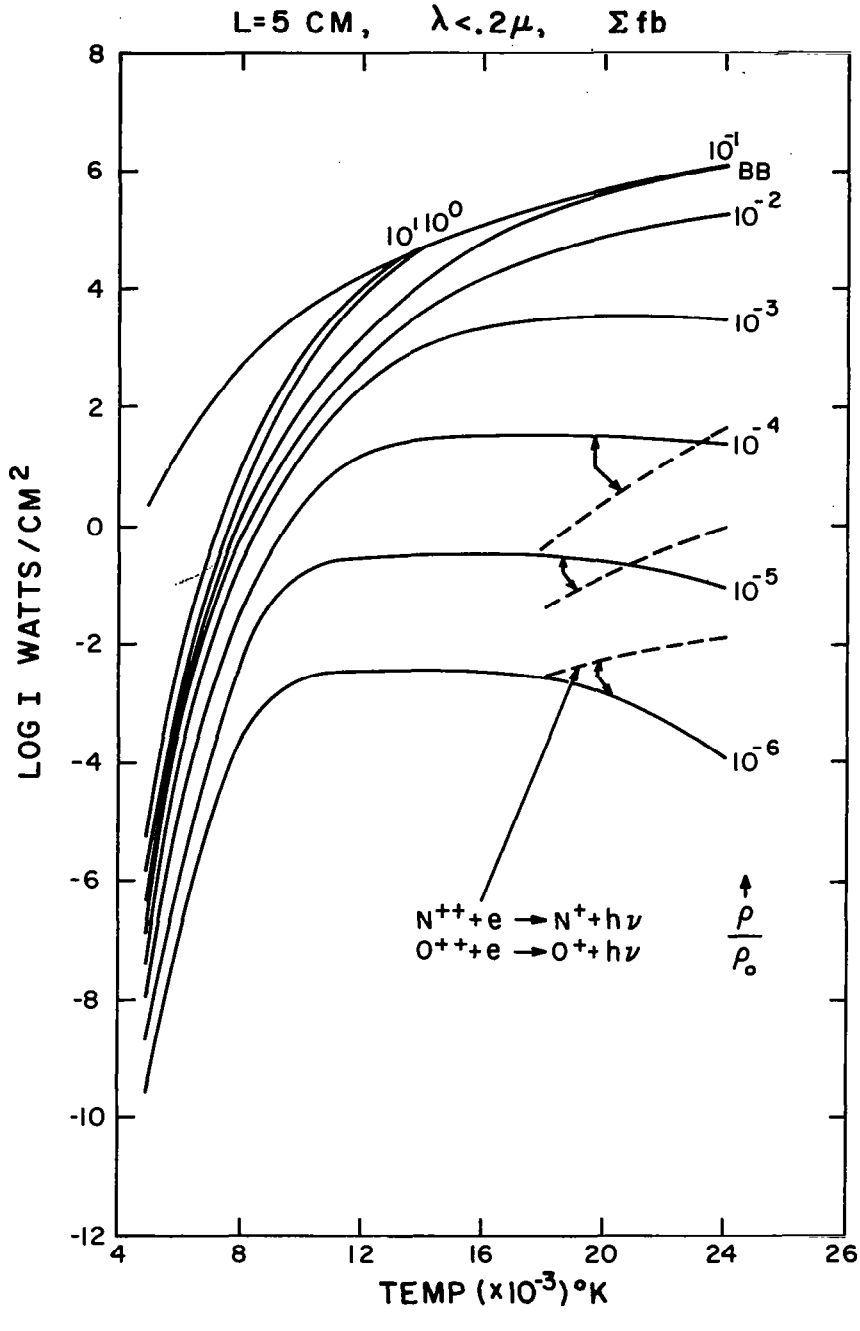


Fig. 19 Nitrogen and oxygen ion free bound radiation flux from one side of an infinite air slab 5 cm thick for wavelengths less than 0.2 $\mu$. The dashed lines are for the contributions from the $N^{++}$ and $O^{++}$.

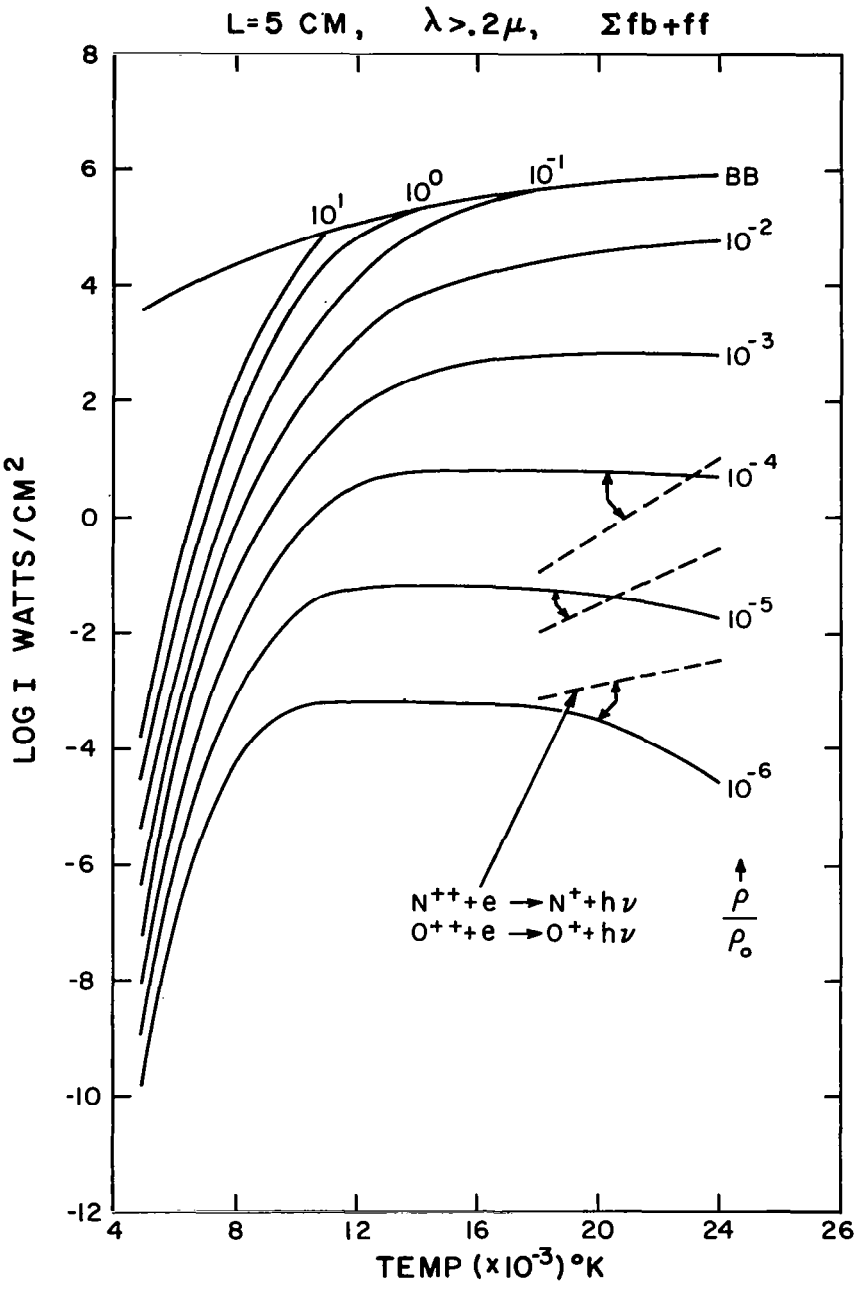


Fig. 20 Nitrogen and oxygen ion free bound and free free radiation flux from one side of an infinite air slab 5 cm thick for wavelengths greater than 0.2 $\mu$. The dashed lines are for the contribution from $N^{++}$ and $O^{++}$.

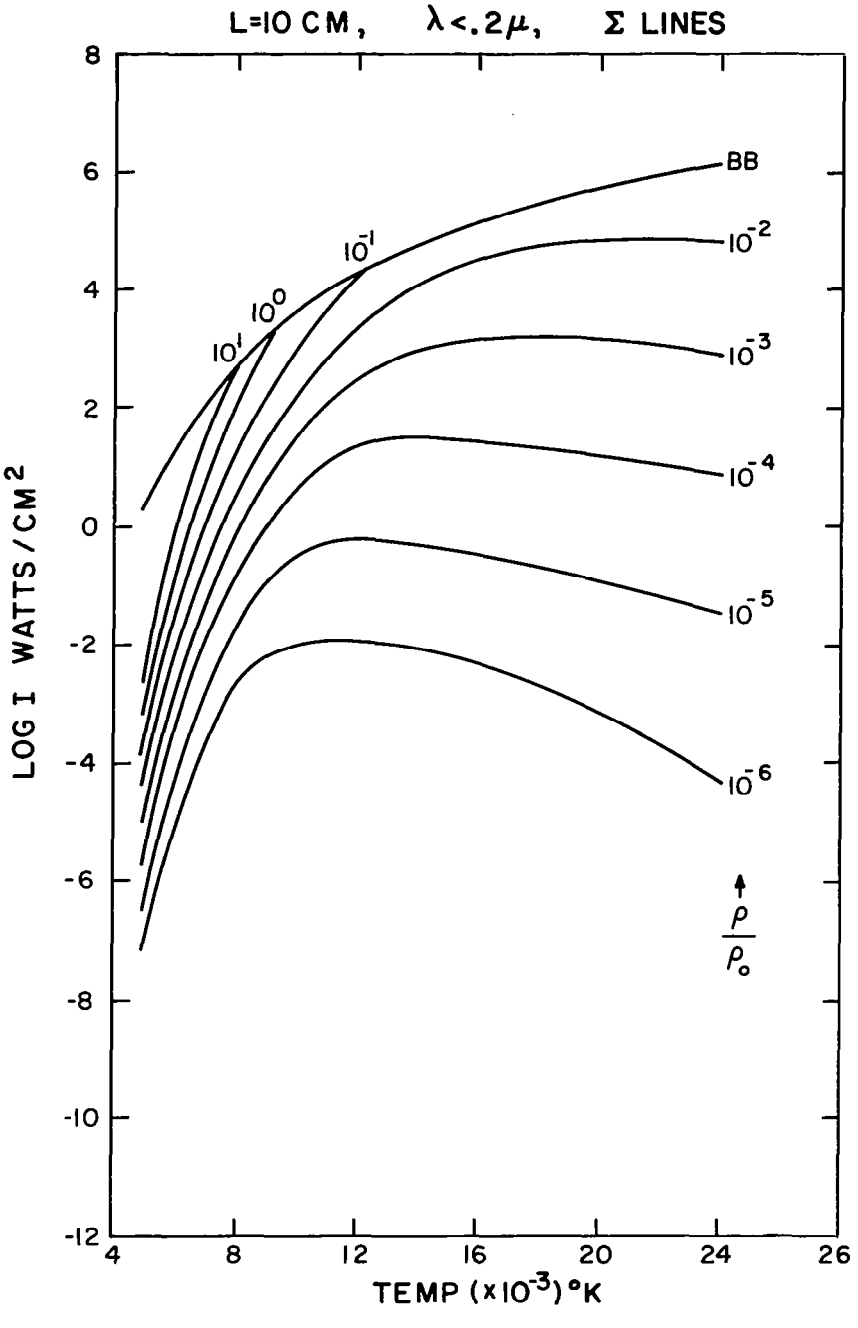


Fig. 21 Atomic nitrogen and oxygen line radiation flux from one side of an infinite air slab 10 cm thick for wavelengths less than 0.2 $\mu$.

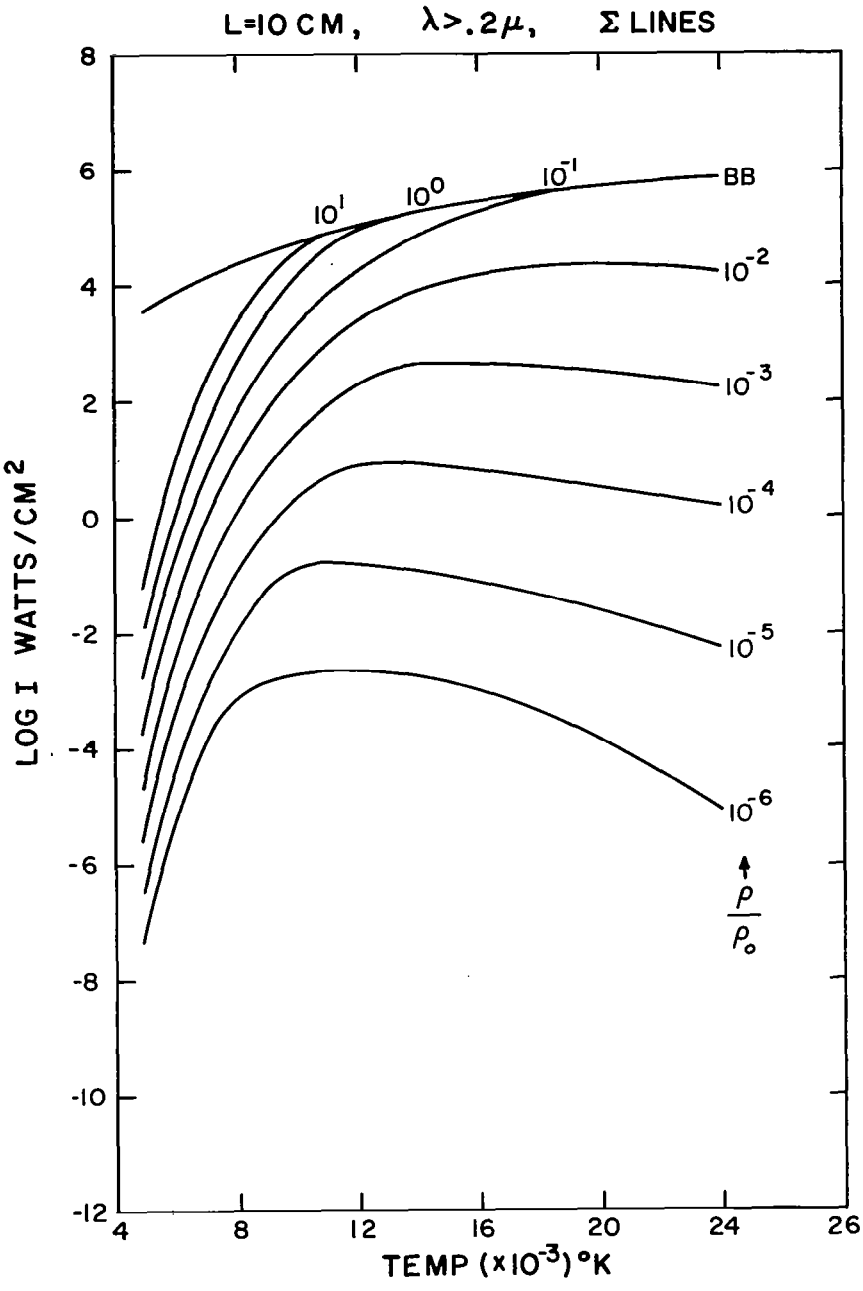


Fig. 22 Atomic nitrogen and oxygen line radiation flux from one side of an infinite air slab 10 cm thick for wavelengths longer than 0.2 $\mu$.

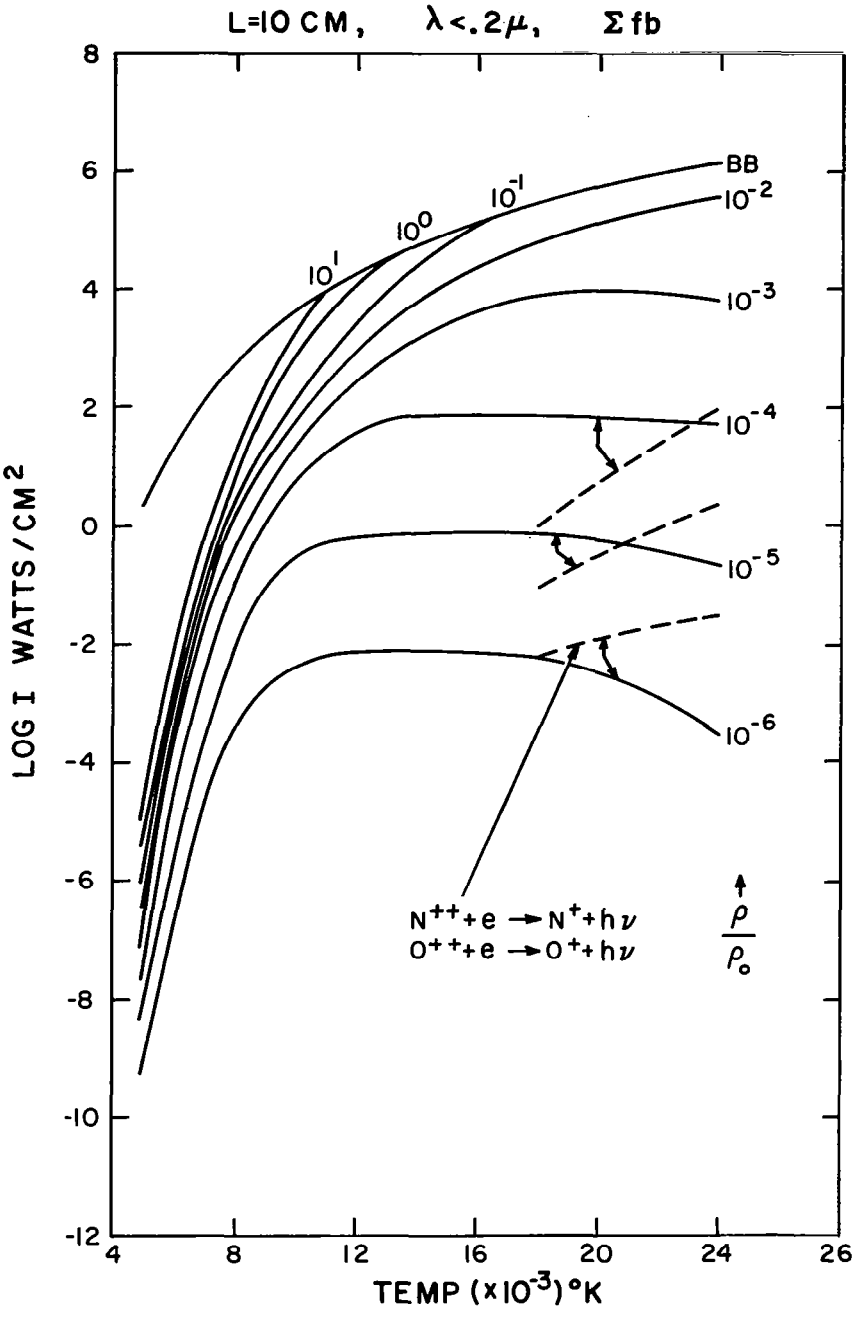


Fig. 23 Nitrogen and oxygen ion free bound radiation flux from one side of an infinite air slab 10 cm thick for wavelengths less than 0.2$\mu$. The dashed lines are for the contributions from the $N^{++}$ and $O^{++}$.

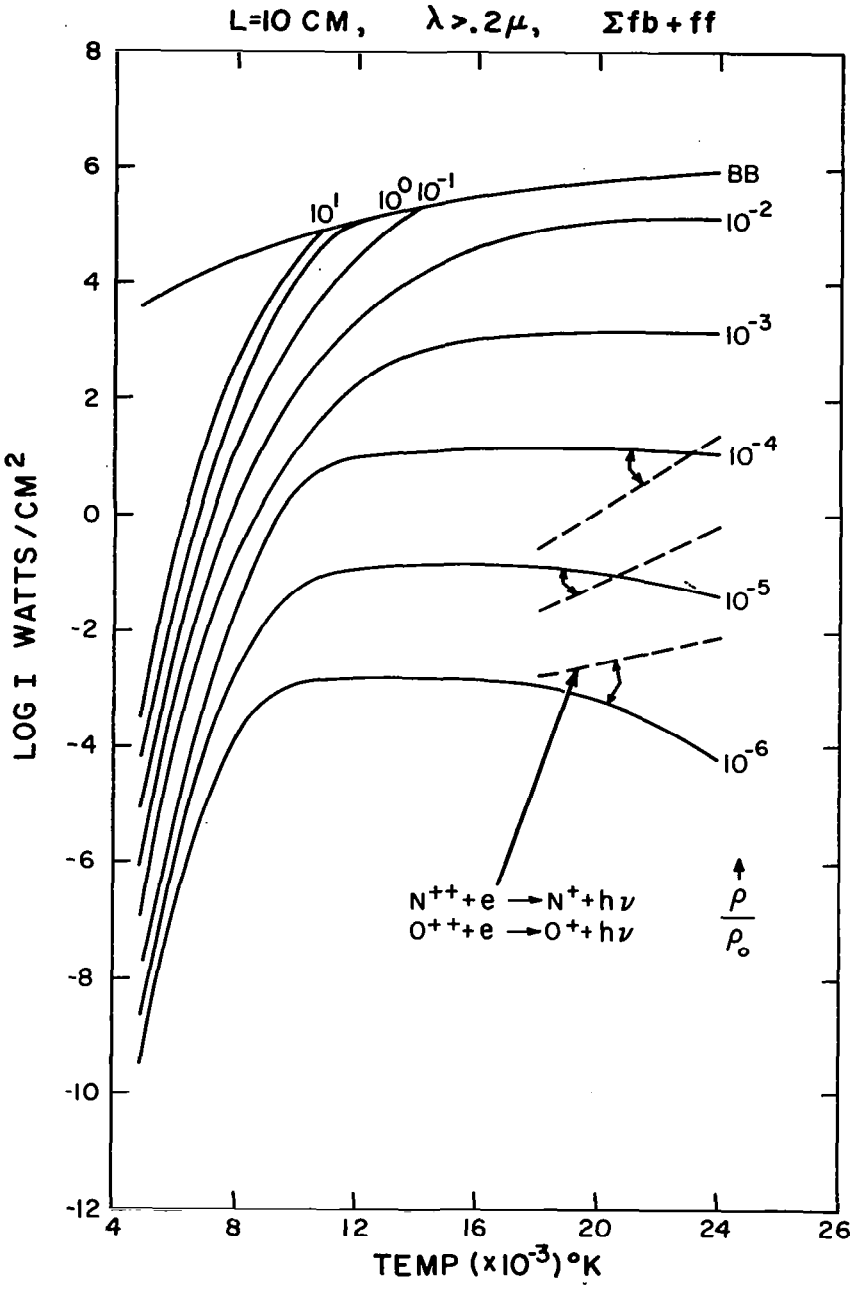


Fig. 24 Nitrogen and oxygen ion free bound and free free radiation flux from one side of an infinite air slab 10 cm thick for wavelengths greater than 0.2 $\mu$. The dashed lines are for the contribution from $N^{++}$ and $O^{++}$.

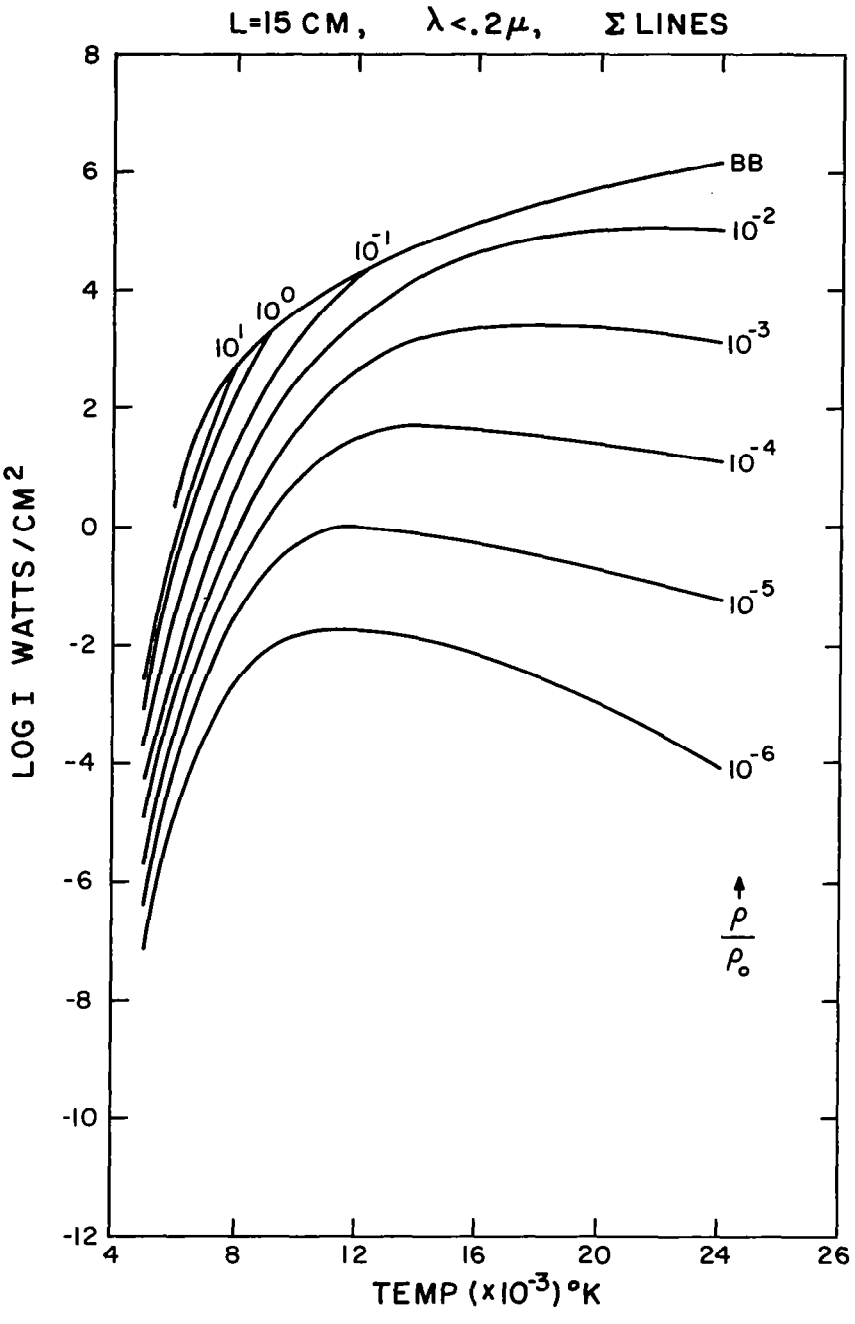


Fig. 25 Atomic nitrogen and oxygen line radiation flux from one side of an infinite air slab 15 cm thick for wavelengths less than 0.2 $\mu$.

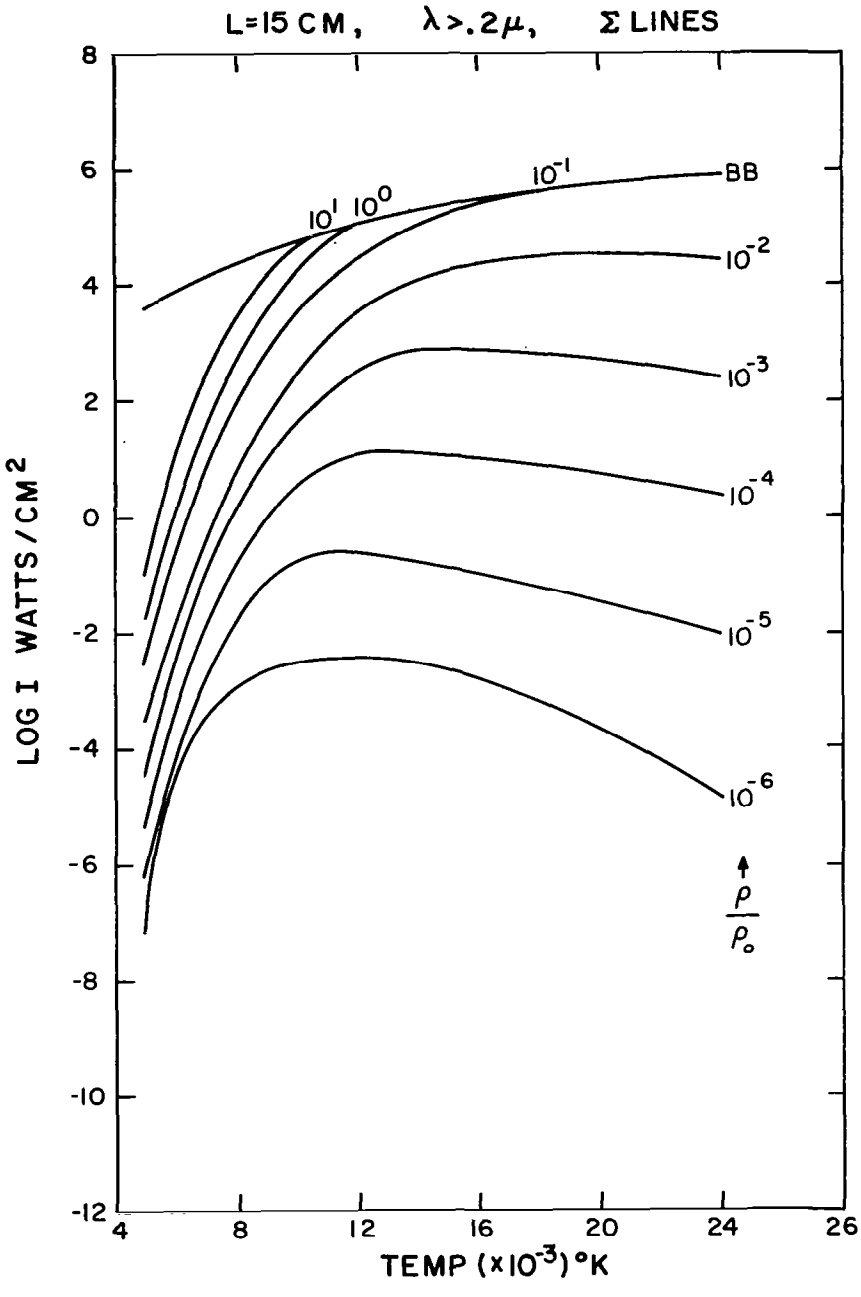


Fig. 26 Atomic nitrogen and oxygen line radiation flux from one side of an infinite air slab 15 cm thick for wavelengths longer than 0.2 $\mu$.

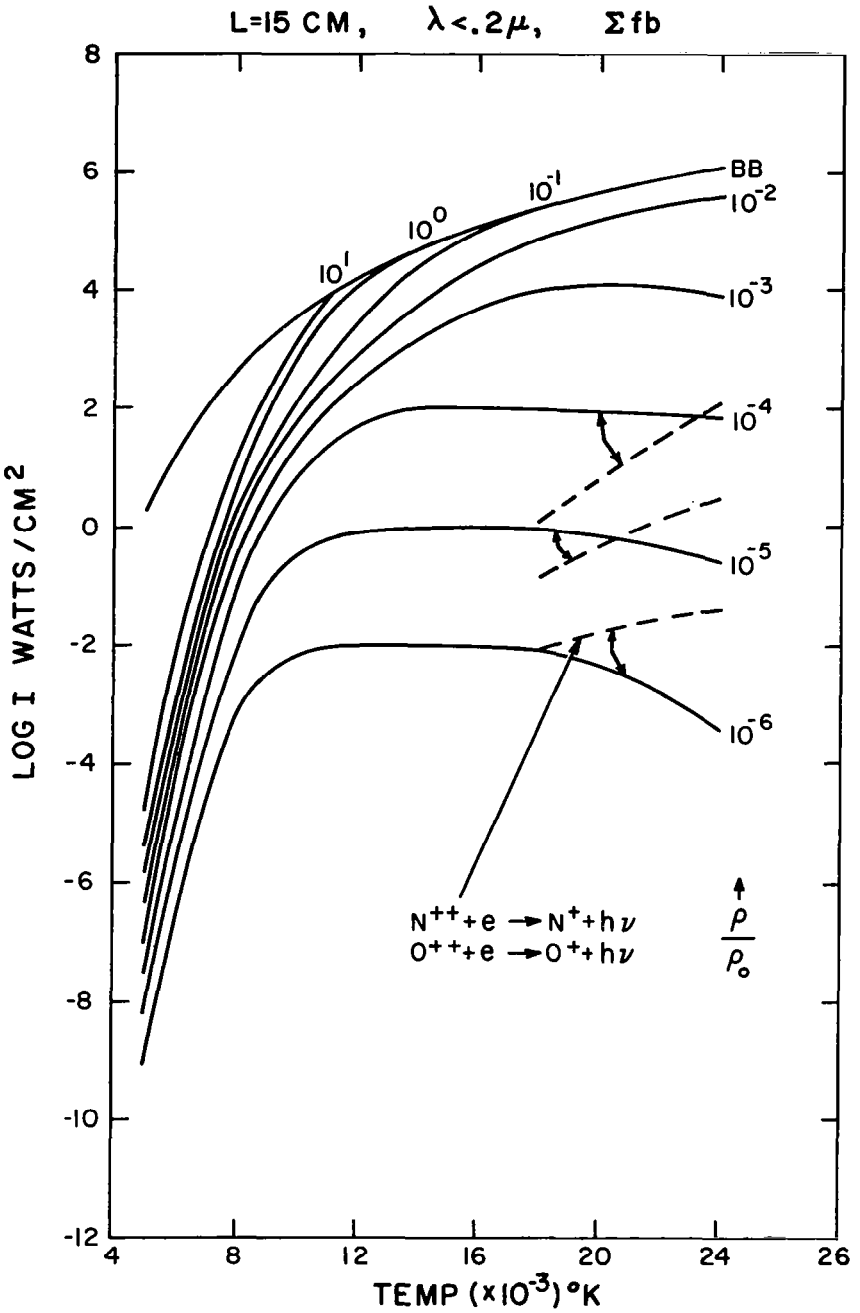


Fig. 27 Nitrogen and oxygen ion free bound radiation flux from one side of an infinite air slab 15 cm thick for wavelengths less than 0.2 $\mu$. The dashed lines are for the contributions from the $N^{++}$ and $O^{++}$.

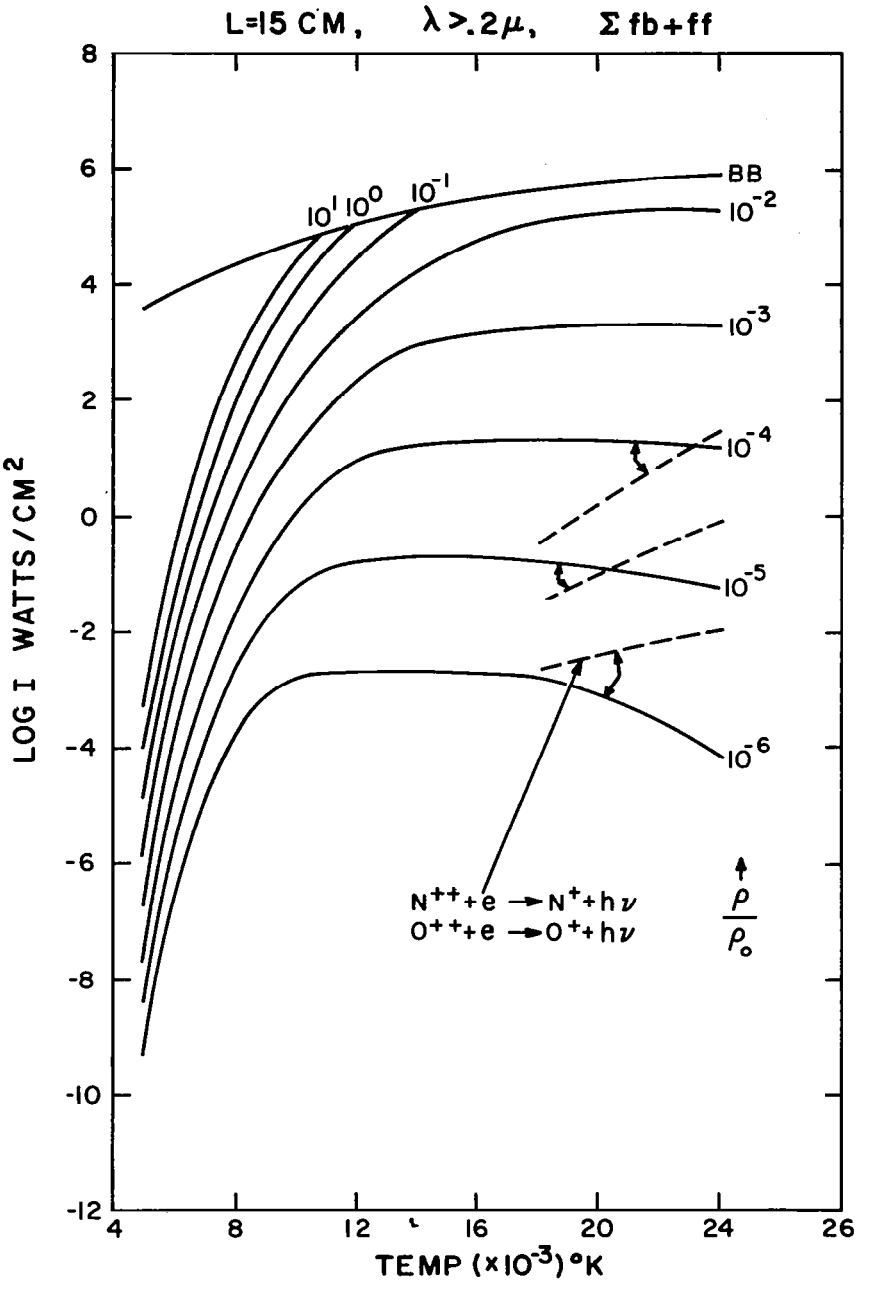


Fig. 28 Nitrogen and oxygen ion free bound and free free radiation flux from one side of an infinite air slab 15 cm thick for wavelengths greater than 0.2 $\mu$. The dashed lines are for the contribution from $N^{++}$ and $O^{++}$.

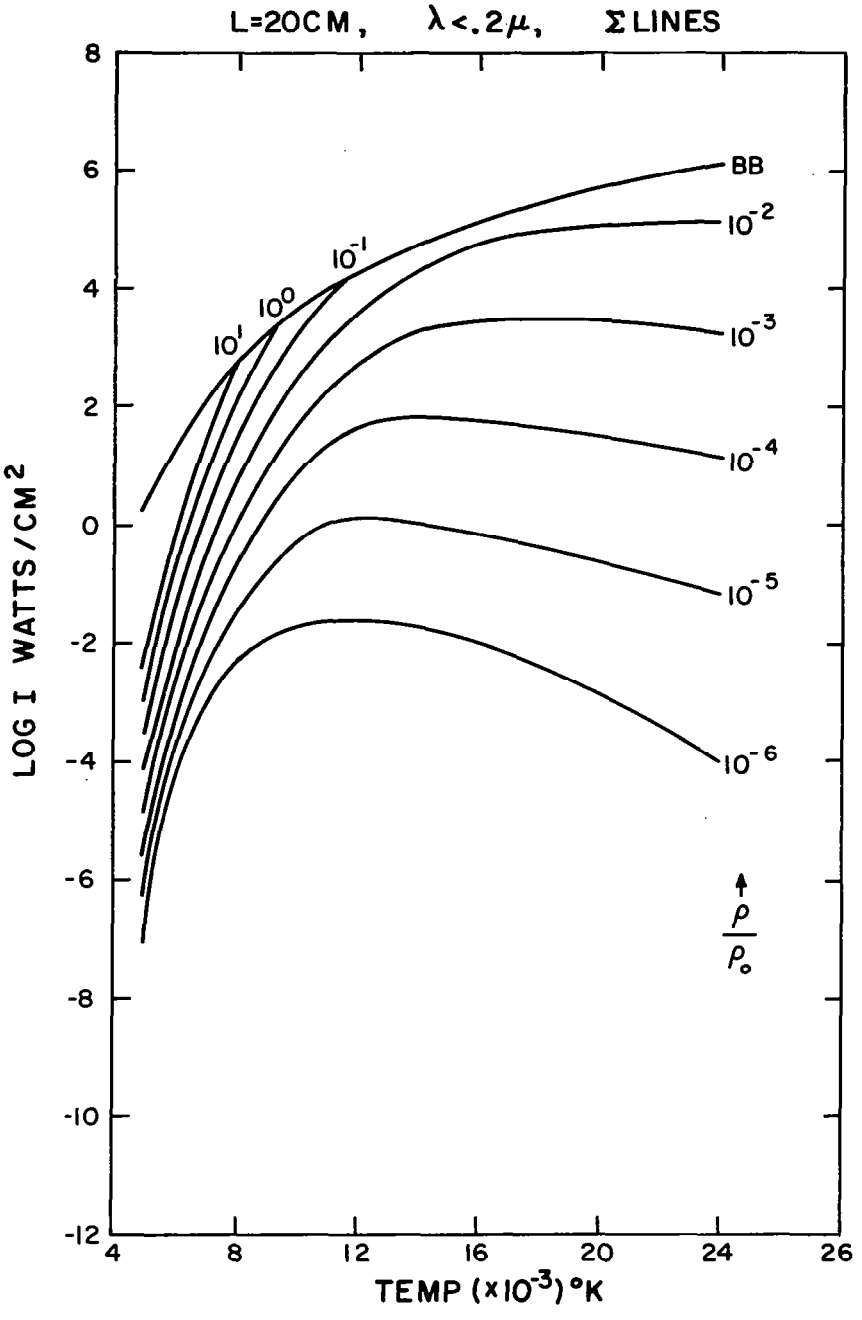


Fig. 29 Atomic nitrogen and oxygen line radiation flux from one side of an infinite air slab 20 cm thick for wavelengths less than 0.2 $\mu$.

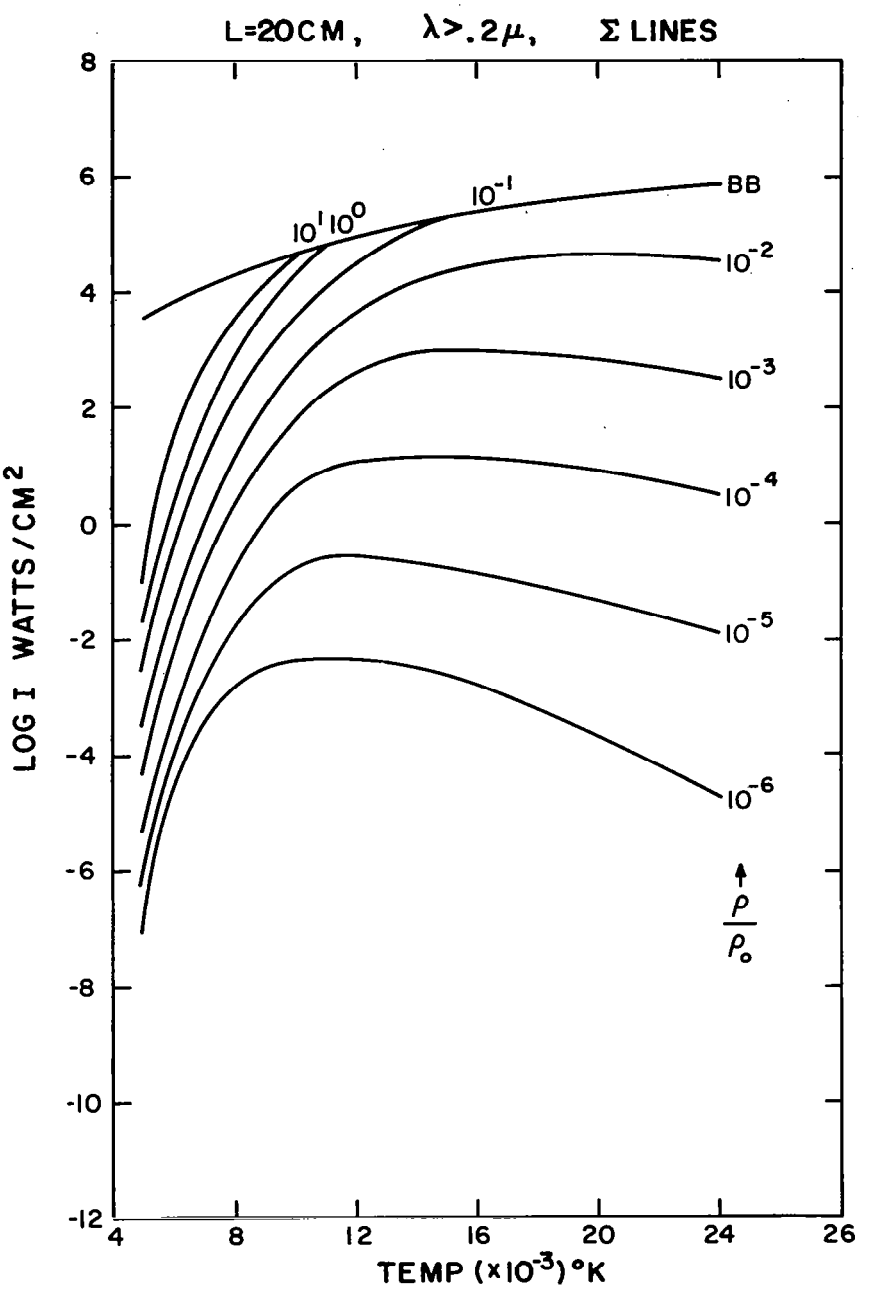


Fig. 30 Atomic nitrogen and oxygen line radiation flux from one side of an infinite air slab 20 cm thick for wavelengths longer than 0.2 $\mu$.

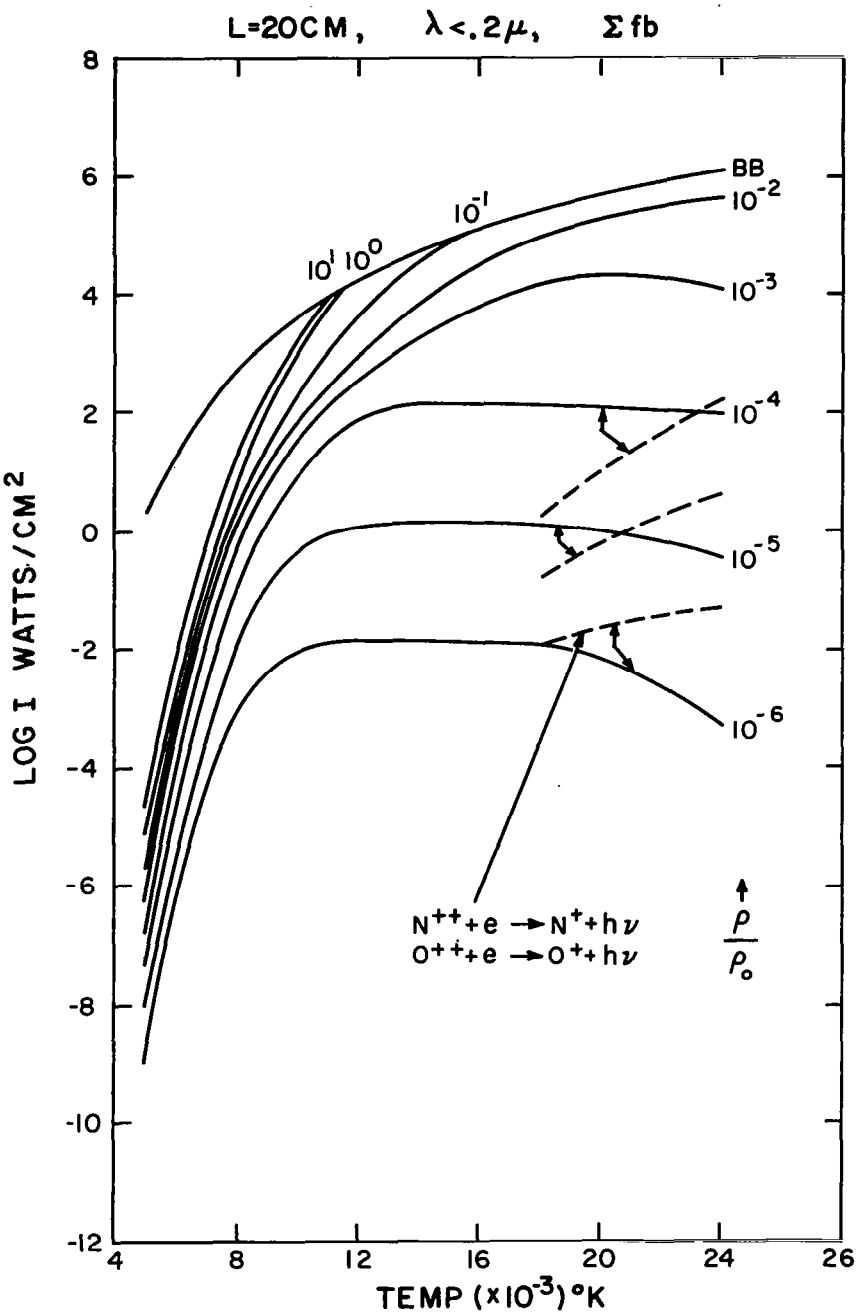


Fig. 31 Nitrogen and oxygen ion free bound radiation flux from one side of an infinite air slab 20 cm thick for wavelengths less than 0.2 $\mu$. The dashed lines are for the contributions from the $N^{++}$ and $O^{++}$.

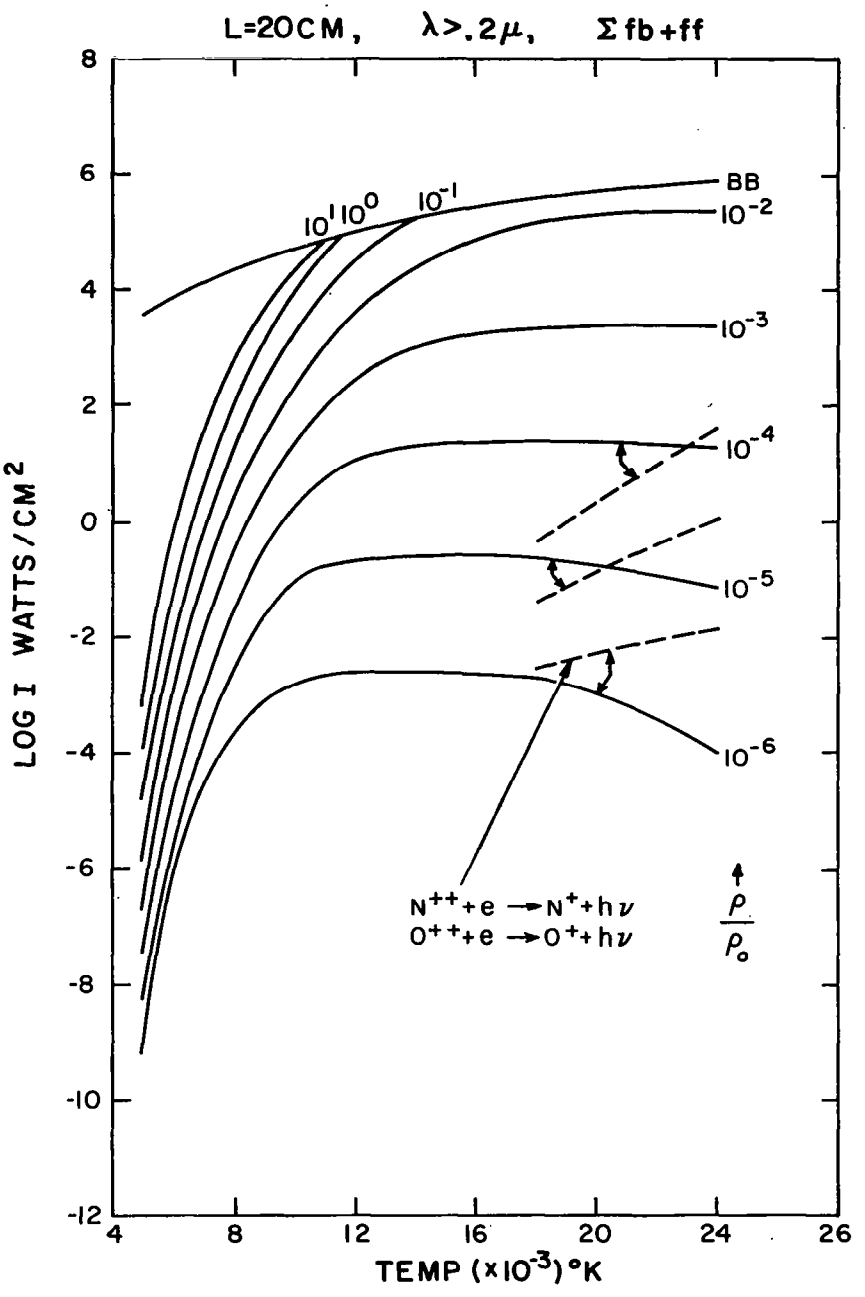


Fig. 32 Nitrogen and oxygen ion free bound and free free radiation flux from one side of an infinite air slab 20 cm thick for wavelengths greater than 0.2 $\mu$. The dashed lines are for the contribution from $N^{++}$ and $O^{++}$.

## REFERENCES


1. Wick, B. H., "Radiative Heating of Vehicles Entering the Earth's Atmosphere," presented to the Fluid Mechanics Panel of Advisory Group for Aeronautical Research and Development, Brussels, Belgium, (April 3 - 6, 1962).

2. Allen, R. A., "Air Radiation Tables: Spectral Distribution Functions for Molecular Band Systems," Avco-Everett Research Laboratory Research Note 560, NASA CR-557.

3. Keck, J., Camm, J., Kivel, B. and Wentink, T., Jr., "Radiation from Hot Air" Part II, Avco-Everett Research Laboratory Research Report 42, Annals of Phys., 7, 1-38 (May 1959).

4. Patch, R. W., Shackleford, W. L. and Penner, S. S., "Approximate Spectral Absorption Coefficient Calculations for Electronic Band Systems belonging to Diatomic Molecules", J. Quant. Spect. Rad. Transf. 2, 263-271 (1962).

5. Keck, J. C., Allen, R. A., and Taylor, R. L., "Electronic Transition Moments for Air Molecules", Avco-Everett Research Laboratory Research Report 149, J. Quant. Spect. Rad. Transf. 3, 335-353 (Oct. - Dec. 1963).

6. Mulliken, R. S., "Intensities of Electronic Transitions in Molecular Spectra", J. Chem. Phys. 7, 14-21 (Jan. 1939).

7. Nicholls, R. W., "Transition Probabilities of Aeronomically Important Spectra", Annals of Phys., 20, 144-181 (April - June 1964).

8. Herzberg, G., Molecular Spectra and Molecular Structure, Vol. I Spectra of Diatomic Molecules (Van Nostrand Co., Inc., New York 1950).

9. Allen, R. A., "Nonequilibrium Shock Front Rotational, Vibrational and Electronic Temperature Measurements", Avco-Everett Research Laboratory Research Report 186, J. Quant. Spect. Rad. Transf. 5, 511, (1965).

10. Fairbairn, A. R., "Shock Tube Study of the Oscillator Strength of the $C_2$ Swan Band", Avco-Everett Research Laboratory Research Note 557, (July 1965).

11. Hilsenrath, J. and Klein, M., "Tables of Thermodynamic Properties of Air in Chemical Equilibrium including Second Virial Corrections from 1500°K to 15,000°K", AEDC-TR-65-58 (March 1965).

12. Gilmore, F. R., "Equilibrium Composition and Thermodynamic Properties of Air to 24,000°K", Rand Corp. RM-1543 (Aug. 1955).

13. Bethe, H. A. and Salpeter, E. E., Quantum Mechanics of One and Two Electron Atoms, New York, Academic Press (1957).

14. Moore, C., "Atomic Energy Levels", Vol. I NBS Circ. 467, (June 15, 1949).

15. Aller, L. H., Astrophysics: The Atmospheres of the Sun and Stars. New York, Ronald Press, pp 122 - 180, (1953).

16. Unsold, A., Ann. Physik 33, 607, (1938).

17. Allen, R. A., Textoris, A., and Wilson, J., "Measurements of the Free-Bound and Free-Free Continua of Nitrogen, Oxygen and Air", Avco-Everett Research Laboratory Research Report 195, J. Quant. Spectr. Rad. Transf. 5, 95-108 (1965).

18. Bates, D. R. and Seaton, J. J., "The Quantal Theory of Continuous Absorption of Radiation by Various Atoms in their Ground States", II. Further Calculations on Oxygen, Nitrogen and Carbon, Monthly Not. Roy. Astro. Soc. 109, No. 6, 698 - 704 (1949).

19. Ehler, A. W., and Weissler, G. L., F. Opt. Soc. Amer. 45, 1035 (1955).

20. Olfe, D. B., "Mean Beam Length Calculations for Radiation from Non-Transparent Gases", J. Quant. Spect. Rad. Transf. 1, 169 - 176.

21. Baranger, M., "Spectral Line Broadening in Plasmas", Vol. 13, Atomic and Molecular Processes, Academic Press, New York, 493 - 548 (1962).

22. Armstrong, B. H., "Broadening of Balmer Lines for High Quantum Number", J. Quant. Spect. Rad. Transf. 4, 491 (May - June 1964).

23. Stewart, J. C. and Pyatt, K. D., Jr., "Theoretical Study of Optical Properties. Photon Absorption Coefficients, Opacities and Equations of State of Light Elements, including the Effect of Lines", Final Report Contract AF 29(601)-2807, General Atomic Division, General Dynamics Corporation (Sept. 1961).

24. Penner, S. S., Qualitative Molecular Spectroscopy and Gas Emmissivities, Addison-Wesley, (1959).

25. Plass, Gilbert N., "Models for Spectral Band Absorption", J. Opt. Soc. Amer. 48, (Oct. 1958).

26. Griem, H. R., Plasma Spectroscopy, McGraw-Hill Book Co., (1964).

27. Stampa, A., Z. Astrophys. 58, 82-92, (1963).

28. Wray, K. L. and Connolly, T. J., "Nitrogen and Air Radiation in the Near IR", Avco-Everett Research Laboratory Research Report 200, J. Quant. Spect. Rad. Transf. 5, 111-123, (1965).

29. Leavitt, B. P., "Temperature and Wavelength Dependence of the Thermal Emission and O - NO Recombination Spectra of $NO_2$", J. Chem. Phys. 42, No. 3, 1038-1047, (Feb. 1965).

30. Branscomb, L. M., Burgh, S. S., Smith, S. J. and Geltman, S., "Phtodetachment Cross Section and the Electron Affinity of Atomic Oxygen", Phys. Rev. 111, 504-513 (1958).

31. Taylor, R. L., "Continuum Infrared Radiation from High Temperature Air and Nitrogen", Avco-Everett Research Laboratory Research Report 154, J. Chem. Phys. 39, 2354 - 2360 (Nov. 1, 1963).

32. Gilmore, F. R., "The Contribution of Generally-Neglected Band Systems and Continua to the Absorption Coefficient of High-Temperature Air", J. Quant. Spect. Rad. Transf. 5, 125 - 135 (Jan - Feb. 1965).

33. Breeze, J. C. and Ferriso, C. C., "Integrated Intensity Measurements of the 5.3-$\mu$ Fundamental and 2.7-$\mu$ Overtone Bands of NO between 1400° and 2400°K", J. Chem. Phys. 41, 3420 - 7 (1964).

34. Wurster, W. H., "Measured Transition Probability for the First-Positive Band System of Notrogen", ARPA Order No. 253-62, CAL Report No. QM-1626-A-3 (Jan. 1962).

35. Wray, K. L. and Teare, J. D., "A Shock Tube Study of the Kinetics of Nitric Oxide at High Temperatures", Avco-Everett Research Laboratory Research Report 95, J. Chem. Phys. 36, 2582-2596, (May 1961).

*"The aeronautical and space activities of the United States shall be conducted so as to contribute . . . to the expansion of human knowledge of phenomena in the atmosphere and space. The Administration shall provide for the widest practicable and appropriate dissemination of information concerning its activities and the results thereof."*

—NATIONAL AERONAUTICS AND SPACE ACT OF 1958

# NASA SCIENTIFIC AND TECHNICAL PUBLICATIONS

TECHNICAL REPORTS: Scientific and technical information considered important, complete, and a lasting contribution to existing knowledge.

TECHNICAL NOTES: Information less broad in scope but nevertheless of importance as a contribution to existing knowledge.

TECHNICAL MEMORANDUMS: Information receiving limited distribution because of preliminary data, security classification, or other reasons.

CONTRACTOR REPORTS: Technical information generated in connection with a NASA contract or grant and released under NASA auspices.

TECHNICAL TRANSLATIONS: Information published in a foreign language considered to merit NASA distribution in English.

TECHNICAL REPRINTS: Information derived from NASA activities and initially published in the form of journal articles.

SPECIAL PUBLICATIONS: Information derived from or of value to NASA activities but not necessarily reporting the results of individual NASA-programmed scientific efforts. Publications include conference proceedings, monographs, data compilations, handbooks, sourcebooks, and special bibliographies.

***Details on the availability of these publications may be obtained from:***

SCIENTIFIC AND TECHNICAL INFORMATION DIVISION

NATIONAL AERONAUTICS AND SPACE ADMINISTRATION

**Washington, D.C. 20546**